Cosmology with Cosmic Voids

Yan-Chuan Cai[,a] and Mark Neyrinck[b]

[a]Institute for Astronomy, University of Edinburgh, Royal Observatory, Blackford Hill
Edinburgh, EH9 3HJ, UK
[b]Blue Marble Space Institute of Science, Seattle, WA, 98104, USA

Glossary

Alcock-Paczynski effect a geometrical distortion in observed galaxy statistics arising from an incorrect cosmological model being used to transform redshift to comoving distance
Baryon Acoustic Oscillations density correlations on ∼ 150 Mpc scales from primordial sound waves
Cosmic Microwave Background light emitted at the surface of last scattering, ∼ 10^5 years after the Big Bang, by now redshifted into the microwave range
Integrated Sachs-Wolfe effect change of photon energy induced by the change of gravitational potentials due to dark energy
Redshift-space distortions distortions to the spatial pattern of galaxies in a galaxy redshift survey, produced by peculiar motions of galaxies
Sunyav-Zel'dovich effect CMB temperature shifts from photons scattering off of plasma
ω, the equation of state of dark energy, defined as the pressure divided by density, $\omega = p/\rho$
Peculiar velocity the velocity of a galaxy on top of the apparent motion from the Universe's expansion
Dark-matter halo a gravitationally-bound clump of dark matter, capable of hosting galaxies if massive enough.
Halo mass function a histogram of dark matter halos of different masses
Two-point statistics describing the excess probability of finding two galaxies separated by a certain distance relative to a random distribution

Nomenclature

AP Alcock-Paczynski effect
BAO Baryon Acoustic Oscillations
BOSS Baryon Oscillation Spectroscopic Survey (large-volume SDSS survey sampling bright galaxies)
CMB Cosmic Microwave Background
DES Dark Energy Survey `https://www.darkenergysurvey.org/`
DESI Dark Energy Spectroscopic Instrument `https://www.desi.lbl.gov/`
ISW Integrated Sachs-Wolfe effect
ΛCDM Our standard cosmological model, with a cosmological constant (Λ) and cold dark matter
RSD Redshift-Space Distortions
SDSS Sloan Digital Sky Survey `https://sdss.org`
(t/k)SZ (thermal/kinetic) Sunyav-Zel'dovich effect
VSF Void Size Function (a histogram of voids with different sizes)
ZOBOV ZOnes Bordering On Voidness (a watershed-based void finder)

Abstract

Cosmic voids are low-mass-density regions on intergalactic scales. They are where cosmic expansion and acceleration are most dominant, important places to understand and analyse for cosmology. This entry summarises theoretical underpinnings of cosmic voids, and explores several observational aspects, statistics and applications of voids. The density profiles, velocity profiles, evolution history and the abundances of voids are shown to encode information about cosmology, including the sum of neutrino masses and the law of gravity. These properties manifest themselves into a wide range of observables, including the void distribution function, redshift-space distortions, gravitational lensing and their imprints on the cosmic-microwave background. We explain how each of these observables work, and summarise their applications in observations. We also comment on the possible impact of a local void on the interpretations of the expansion of the Universe, and discuss opportunities and challenges for the research subject of cosmic voids.
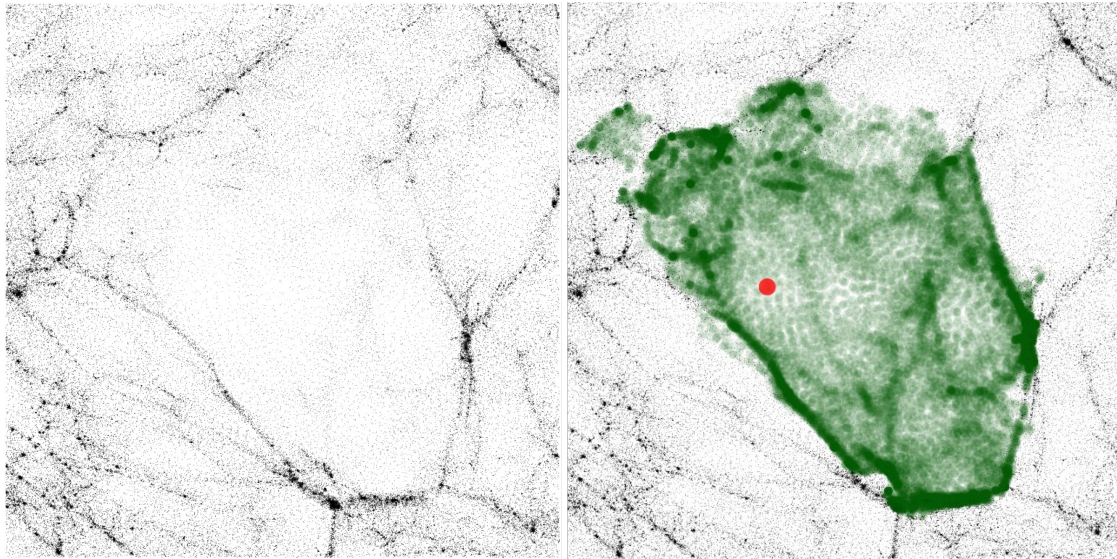
Fig. 1 Left: The matter in a region of the Millennium simulation (Springel et al., 2005) that contains a large void. Black regions are where matter concentrates, and white regions represent low densities. We can see a large, low-density region near the middle, surrounded by irregularly shaped higher-density boundaries. Colour-coded in green on the right-hand panel is the volume identified as a void by the watershed based void-finding algorithm ZOBOV, the red-dot represents the void centre, chosen to be the lowest density point (Neyrinck, 2008; Colberg et al., 2008). The image shows a $(40 \text{ Mpc/h})^2$ region with a thickness of 5 Mpc/h from the simulation. This figure is taken from (Colberg et al., 2008).

1 The key points about cosmic voids

• Cosmic voids are large under-dense regions found in the large-scale matter distribution of the Universe. The lowest matter densities in the Universe are found there, reaching several orders of magnitude lower than the mean density of the Universe, but not all the way to zero. There are various ways to define voids; depending on the definition, they may be entirely devoid (empty) of galaxies, or simply have a lower galaxy number density than their surroundings. Voids are one of four major components of the large-scale structure of the Universe, which consists of voids, walls, filaments and knots. These are organised in complex web-like structures, called the cosmic web. Figure 1 gives an example of a void embedded in the cosmic web from a cosmological simulation.

• The first discovery of cosmic voids went together with the discovery of the cosmic web. Before their discovery in the 1970s, people were aware of the existence of galaxies and galaxy clusters, and that the Universe was expanding, but the spatial distribution of galaxies and galaxy clusters on large scales was largely unknown. In 1978, two independent studies using different surveys of galaxies came to the same conclusion that intergalactic voids exist. Jõeveer et al. (1978) and in Gregory and Thompson (1978) concluded that 'Unexpected in our results are the large dimensions of holes ranging from some ten to hundreds of megaparsecs' (Jõeveer et al., 1978). In the meantime, it was explicitly pointed out that 'there are large regions of space with radii $r > 20$ Mpc where there appear to be no galaxies whatever.' These established the first observational evidence for cosmic voids, and their connection to the cosmic web.

• The density within voids is generally of order 10% of the mean density of the Universe, but voids often contain sub-cosmic webs themselves (Aragon-Calvo and Szalay, 2013; Jaber et al., 2024), with substantial density fluctuations. The effective radius of a void spans from a few Mpc/h to the order of 100 Mpc/h. The majority of the volume of the Universe is filled with voids. According to several major void finding algorithms , the total volume occupied by voids accounts for over 60% of the total volume of the late-time Universe (Cautun et al., 2014; Libeskind et al., 2018). Matter around void centres moves away from them. The boundary of a typical void expands at a faster rate than the expansion of the Universe.

• The statistical properties of voids are dictated by the initial conditions of the Universe. In the standard ΛCDM model, these are set by the cosmological parameters of the model. More directly than for other parts of the universe, the evolution of cosmic voids is shaped by cosmic expansion and global dynamics. Cosmic voids therefore contain information about cosmology and astrophysics. Among them, the density profiles of voids and volume distribution function can be used to measure the sum of neutrino masses, test theories of gravity, and
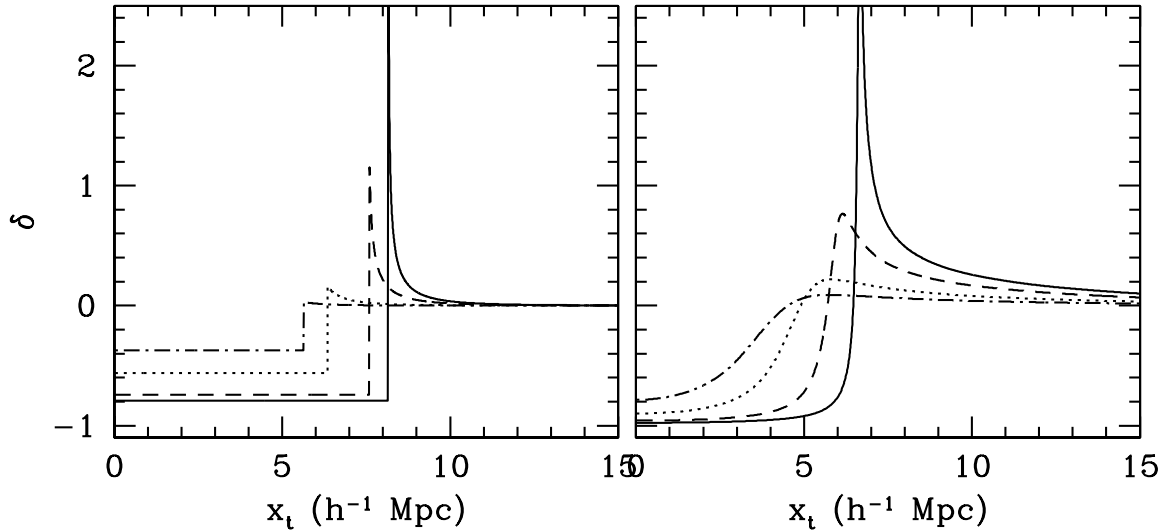
Fig. 2 The evolution of the void density profile from its initial conditions to shell-crossing, in two idealized cases: that of a spherical top-hat under-density (left), and a void with an averaged profile in the SCDM (standard Cold Dark Matter, with $\Omega_m = 1$) model (BBKS, Eq. 7.10) (Bardeen et al., 1986). Different line styles represent different epochs of the Universe with scale factors $a = 0.05$ (dash-dot line), 0.1 (dotted line), 0.2 (dashed line) and 0.3 (solid line). We can see that the voids become emptier as they expand, with matter accumulating at the edge at late epochs, forming high density boundaries. The figure is taken from Figure 3 of (Sheth and van de Weygaert, 2004), see also Figure 6 of the review article van de Weygaert (2016).

constrain cosmological parameters.

• Cosmic voids are emerging as a major cosmological probe. Analysis of galaxy redshift surveys alone has detected redshift-space distortions (Kaiser, 1987) and the Alcock-Paczyski effect (AP) (Alcock and Paczynski, 1979) around voids. Adding additional data, such as the cosmic microwave background (CMB) emitted soon after the Big Bang, and background galaxies, has allowed detection of gravitational lensing and the integrated-Sachs-Wolfe effect (Sachs and Wolfe, 1967). All these have been used to constrain the strength of clustering of matter in the Universe, the rate by which matter perturbations grow, and the matter-energy content of the Universe.

2 The evolution of individual voids

2.1 The formation of voids in a nutshell

According to the standard model of the Universe, our Universe began in a hot and dense state, with matter almost perfectly uniformly distributed. Matter clumps such as galaxies were not to be found. There were, however, small density fluctuations thought to be seeded from quantum fluctuations during the phase of inflation, which was well within the first second after the Big Bang (Guth, 1981; Albrecht and Steinhardt, 1982; Linde, 1983). The fluctuations seeded from inflation developed into small ripples of low and high densities on the order of 1 part in 10^5 in the matter distribution when the CMB was emitted. Driven by the universal gravitational attraction of gravity, these fluctuations continued to grow. Matter continuously moves away from underdensities and flows towards overdensities. The underdense regions grew more and more under-dense, and eventually grew to be (nearly) empty of matter, in regions that now call cosmic voids.

Individual voids have complex and irregular morphologies, such as the one shown in Figure 1. Voids are often idealized as convex polyhedra produced in a Voronoi tessellation (Icke and van de Weygaert, 1991), which has theoretical justification (Hidding et al., 2016; Neyrinck et al., 2018). Physically, voids can be thought of as bubbles in a foam (Aragon-Calvo, 2023) with an interior expansion faster than the cosmic mean. Where they run into each other, they produce the cosmic web of walls, filaments and galaxies.

Dark energy, if conceived as a physical substance, is thought to have constant density throughout the Universe, so voids, where there is very little matter, are the most dark-energy-dominant regions of the Universe. There have even been suggestions that the conditions in voids are crucially responsible for the accelerated expansion we see (e.g. Wiltshire, 2009; Rácz et al., 2017). But the mainstream picture is that a sufficiently good approximation to the dynamics and for observations, even in voids, uses Newtonian gravity on top of an expanding background given directly by cosmological parameters (e.g. Kaiser, 2017).
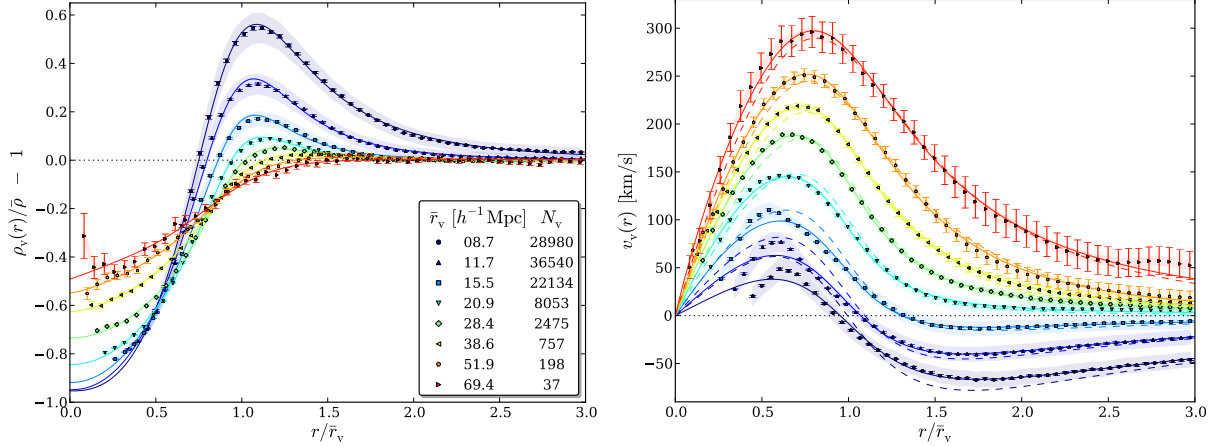
Fig. 3 The averaged density (left) and velocity (right) profiles of voids from cosmological N-body simulations. The averaged size of voids in each bin is represented by their effective radius $\bar{r}_v$, with N_v indicating the number of voids in each bin. We can see that small voids tend to have high and steep density at their edges, while large voids have gentle density boundaries. The interior of voids has positive radial velocities – they are expanding. At large radii, large voids are also expanding, but small voids are contracting, having negative velocities at large radii. Solid lines represent the best-fit solutions from equation 2 for the density and its corresponding velocity profiles by assuming linear coupling between density and velocity. Dashed lines show the linear theory predictions obtained from evaluating the velocity profile equation at the best-fit parameters obtained from the density stacks. The figure is taken from Figure 1 of Hamaus et al. (2014b).

2.2 The spherical expansion model of voids

Although voids have irregular shapes, the average of a large sample of them can be approximated by a spherical underdensity. Spherical symmetry is also relevant because a void (at least, its inner density contours) tends to become more spherical as time passes (Icke, 1984). A spherical model has proven quite useful to understand their dynamics.

The spherical evolution model was initially introduced to understand the evolution and collapse of high-density regions, or dark matter haloes (Bertschinger, 1985; Blumenthal et al., 1992; Sheth and van de Weygaert, 2004). But it can be applied to any spherically symmetric system, including voids. The model assumes that a void starts from a 3D spherical underdensity embedded in an infinite background at the mean density. The assumption of spherical symmetry reduces the 3D problem to that of a 1D density profile. Two examples are shown in Figure 2. According to Gauss' Law, the acceleration of a spherical matter shell at the radius r is solely governed by the total mass within r, and the background dark energy density ρ_Λ, as given by the following equation:

$$\frac{\ddot{r}}{r} = -\frac{4\pi G}{3}\left[\rho_m + (1 + 3w)\rho_\Lambda\right]. \tag{1}$$

ρ_m is the mean total matter density within r; ρ_Λ is the background dark energy density, w is the equation of state of dark energy, G is the gravitational constant; $\dot{r}$ represents the time derivative, or velocity, and so $\ddot{r}$ is the acceleration. The above equation can be solved when the boundary conditions are specified. If the initial density of the void is indeed smaller than the mean density of the Universe, such as a spherical top-hat underdensity within the void radius r_v, as illustrated in Figure 2, the underdensity will expand faster than the Hubble expansion. The matter shells immediately outside r_v expand slower than the matter shell at r_v. This causes matter to build up at the boundary of the void at a later epoch, forming a high-density ridge. The expansion of the inner shell of the void will eventually overtake the outer shell. This is defined as shell crossing for voids. In a matter-dominated Universe with the matter density parameter $\Omega_m = 1$, this happens when the radius of the underdensity expands by a factor of 1.7. With mass conservation, we can find that the density contrast of the evolved top-hat void is $\delta = -0.8$. These values have little dependence on cosmology (Sheth and van de Weygaert, 2004; Demchenko et al., 2016). The mean density of the spherical top-hat void at shell-crossing has been taken as a conventional definition for voids.

With a smoother initial density profile such as the one illustrated at the right-hand panel of Figure 2, the evolution of the void density profile is qualitatively similar to the case of the spherical top-hat profile except that the density ridge at the boundary of the void is smoother. The inside of the void is in a sense pristine, with various things preserved from the initial conditions: its initial void density profile is partly preserved, as is even its primordial fluctuation pattern (Aragon-Calvo and Szalay, 2013; Neyrinck and Yang, 2013; Neyrinck et al., 2022) at a later epoch. This in principle allows us to use the observed profile of voids at late times to constrain the initial conditions of the Universe, and therefore measure the cosmological parameters of a model universe.

Testing against measurements from cosmological simulations, the spherical evolution model has been shown to be a reasonable approximation in tracking the evolution of the density profiles of large voids, but it fails for smaller voids (Demchenko et al., 2016). It was pointed out that it was important to account for the peculiar motions of individual voids for the model (Massara and Sheth, 2018). It was recently shown (Verza et al., 2024) that by using an effective moving barrier, adjusting the density field with respect to the void formation threshold, the predicted Lagrangian void density profiles can match up with measurements from cosmological simulations.

The spherical model and its variants provide us with physical intuitions for the evolution of voids on average – that voids are expanding relative to the background Universe. They also provide the basis for deriving analytical expressions for the distribution function of the sizes of voids. The shell-crossing definition of a void boundary can be useful beyond the idealised spherical model, with aspherical or even non-convex boundaries (Falck et al., 2014).

2.3 The density profiles of voids

There has not been a first-principle derivation for the density profiles of voids, but an empirical fitting formulate with free parameters was found in simulations (Hamaus et al., 2014b). It provides good descriptions for the average profiles of voids at low redshifts (see the left-hand panel of Figure 3),

$$\delta(r) = \delta_c \frac{1 - (r/r_s)^\alpha}{1 + (r/r_v)^\beta},\tag{2}$$

where $\delta(r) = \rho(r)/\bar{\rho} - 1$ is the density contrast with respect to the background density of the Universe. The parameters are: δ_c – the density contrast at the void centre; r_v – the effective radius of the void; r_s – a scale radius at which the density of the void equals to the the mean density of the Universe; two power-law indices α and β that control the inner and outer slopes of the void profile. The formula applies for voids found with the ZOBOV algorithm (Neyrinck, 2008). We can see from Figure 3 that it fits well the density profiles of the voids with a wide range of void radii. In addition, it was demonstrated that the mean peculiar velocities around these voids follow the predictions from linear theory reasonably well i.e., the radial velocity profile $v(r)$ around the void centre, and the density perturbation within the radius r, $\bar{\delta}(r)$, are linearly coupled by constant factors:

$$v(r) = -\frac{1}{3}raH(a)\bar{\delta}(r),\tag{3}$$

where

$$\bar{\delta}(r) = \frac{3}{r^3}\int_0^r \delta(r')r'^2 dr'\tag{4}$$

(see the right-hand panel of Figure 3). For voids with a wide range of radii, they all exhibit positive radial velocities inside the void radius, indicating that voids are expanding relative to the expansion of the Universe. The dynamically simple nature of voids is an advantage of voids compared to high-density regions because they better preserve cosmological information from the initial conditions. This is one reason for the large amount of cosmological information one can obtain using observations of cosmic voids.

2.4 Applications

We can see from the equation of spherical evolution that the strength of gravity (via G) and the property of dark energy (via w) affect the evolution of the voids. In addition, neutrinos, which gravitate but were relativistic in the early Universe and have streaming velocities (Szalay and Marx, 1976), also play a different role in shaping the evolution of voids. The late-time density profiles of voids, which we can observe, carry the imprints of neutrinos. This allows us to use the profiles of voids to test theories of gravity, constrain dark energy and the properties of neutrinos.

For theories of gravity which predict coupling between the strength of gravity with the matter density, such as $f(R)$ gravity (Hu and Sawicki, 2007), the impact of modified gravity on structure formation can be stronger in voids. Voids are made emptier by the fifth force in this model compared to their counterparts in general relativity (Cai et al., 2015; Perico et al., 2019). A Similar effect is found for the nDGP models (Paillas et al., 2019).

For neutrinos, due to their streaming velocities, they do not cluster as strongly as cold dark matter. In voids, their mass ratio against dark matter may be relatively high, and as the size of voids may be comparable to the scale of free-streaming of massive neutrinos (Zhang et al., 2020), we may expect a stronger impact of neutrinos on the growth of structure around voids. Indeed, studies using cosmological *N*-body simulations show that voids in massive neutrino cosmologies are less empty compared to the case of no neutrinos (Massara et al., 2015; Kreisch et al., 2019). This can potentially be detected with gravitational lensing (Vielzeuf et al., 2023). Neutrinos, although they have a small mass fraction, can be thought of as hot dark matter; similarly to the above, voids in a model with warm instead of cold dark matter are usually shallower density depressions (Yang et al., 2015).

The ellipticity of voids has also been proposed as a probe for the dark energy equation of state (Lee and Park, 2009; Lavaux and Wandelt, 2010; Bos et al., 2012; Sutter et al., 2015).

3 The distribution function of voids

Given a sample of voids, making the histogram of their number counts according to their sizes yields the distribution function of voids, or the VSF. The size of a void is characterised by its volume V, or the effective radius, r_v according to $r_v = [3V/(4\pi)]^{1/3}$. Examples of a VSF are shown in Figure 3, where typically small voids are more abundant than large ones.

In the literature, the distribution function of voids can be named differently. It can be called the void probability function (VPF), or the void abundance function. It was shown in White (1979) that the void probability function, defined in the paper as the probability of a randomly placed region of a given volume being empty, is strongly influenced by correlations of all orders. The VSF therefore includes
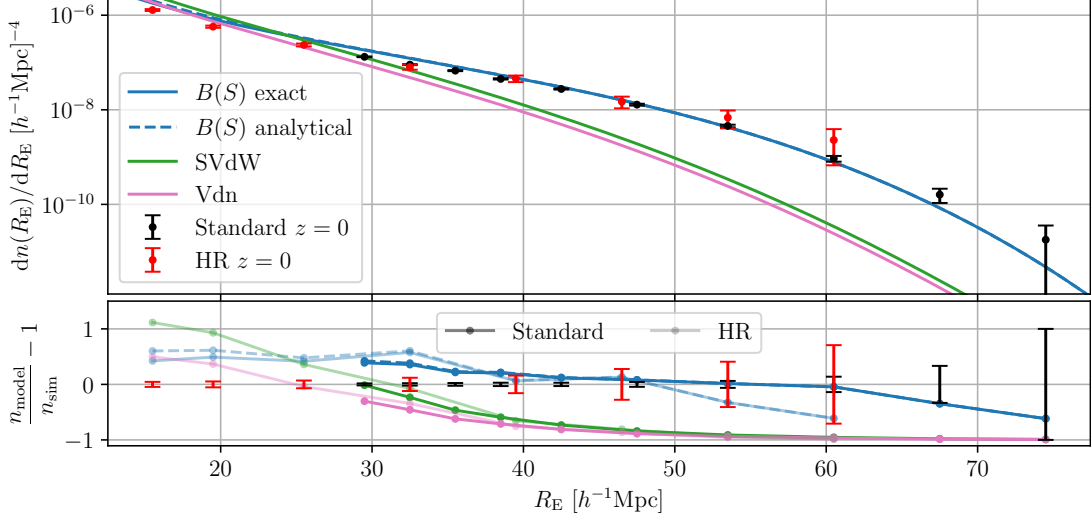
Fig. 4 Top panel: the distribution function of void sizes (VSF) measured from cosmological N-body simulations (black data points with errors and red data points with errors) at $a = 1$. The y-axis indicates the number density of voids per unit volume per unit void radius R_E (x-axis). The blue solid and dashed lines show the best-fit model presented in Verza et al. (2024) and its analytical approximations. The model of Sheth and van de Weygaert (2004) (SVdW) and its renormalised version (Vdn) (Jennings et al., 2013) are shown in green and pink lines. Bottom panel: relative difference between the theoretical models in the upper panel with respect to the measurements from simulations. The figure is taken from Figure 4 of Verza et al. (2024). Here, the Eulerian formation barrier of voids is chosen to be $\delta_v^E = -0.409$, corresponding to the Eulerian linear barrier $\delta_v^{Lin} = -0.623$.
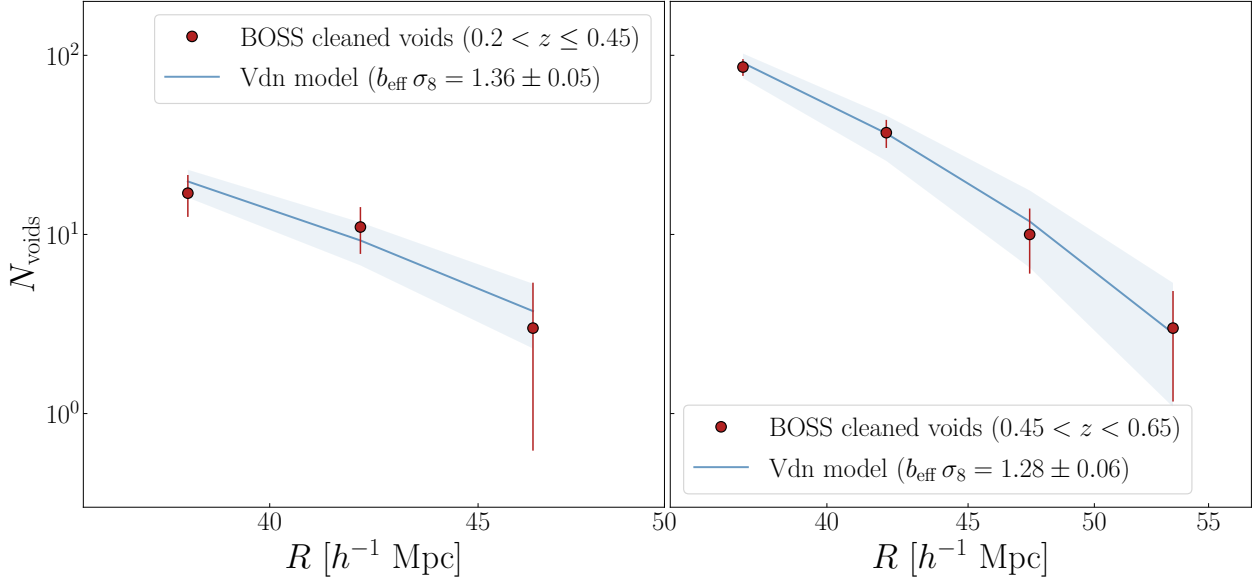

Fig. 5 Top panel: the size distribution function of voids (VSF) measured with voids found in the SDSS-BOSS-DR12 (Sloan Digital Sky Survey – Baryon Oscillation Spectroscopic Survey – Data Release 12) galaxy sample (red data points with errors) at two different redshift bins shown in the legend. The best-fit model is the Vdn model (Jennings et al., 2013), which is the renormalised SVdW (Sheth and van de Weygaert, 2004) model, and is extended with two extra nuisance parameters. Priors informed from calibrations with mocks are used for the nuisance parameters in the fit. They are marginalised over for obtaining the order of 10% measurements for cosmological parameters of matter density Ω_m, amplitude of fluctuations σ_8 and the dark energy equation of state w (Contarini et al., 2023). The figure is taken from Figure 5 of Contarini et al. (2023).

some cosmological information beyond two-point statistics. It can be used to measure cosmological parameters, including the sum of neutrino masses, and test theories of gravity. For these applications, it is necessary to have theoretical predictions for the VSF.

The VSF is fundamentally connected to the initial conditions and evolution of the individual voids mentioned in the previous section. Analytical predictions for the VSF are usually based on the excursion set theory (Bond et al., 1991) in conjunction with the spherical evolution model. Provided with the initial density fluctuations, which are assumed to be Gaussian, the excursion-set theory predicts the probability of initial under-dense regions to form voids in the late-time Universe. The basic idea is that a sequence of density fluctuations $\delta(S)$ with increasing S follows a Brownian random walk, if the filtering of the density field is a Fourier k-space top-hat (Bond et al., 1991; Sheth and van de Weygaert, 2004; Zentner, 2007). $S = \sigma^2(R_i)$ is the variance of the initial density field smoothed by a top-hat filter of radius R_i; in the several-Mpc regime of interest, increasing S means decreasing R_i. A random walk that first down-crosses the void formation barrier δ_v is counted as a void. The probability density of a walk first crossing the barriers between $[\sigma, \sigma + d\sigma]$ is expressed as:

$$\frac{df(\sigma, \delta_v)}{d\ln\sigma} = \frac{\delta_v}{\sigma} \sqrt{\frac{2}{\pi}} \exp\left(-\frac{\delta_v^2}{2\sigma^2}\right),$$ (5)

where $\delta_v = -2.81$ is the linearly extrapolated density to the time of shell-crossing. The corresponding depth of the non-linearly evolved void is $\delta_{NL} = -0.8$. This was first derived in (Sheth and van de Weygaert, 2004).

The above excursion set theory was initially developed for predicting the halo mass function. However, applying it to voids leads to violation of volume conservation. This is because voids expand as they evolve. By the time of shell-crossing, its radius would have grown by a factor of 1.7, as mentioned in the previous section, and so their volume would have grown by a factor of ~ 5. The sum of the volumes of voids at the late-time Universe exceed their total initial comoving volume. An improved version of the model was derived in (Jennings et al., 2013) by imposing volume conservation, which predicts the number density of voids dn per unit logarithmic radius bin $d\ln r_v$ to be:

$$\frac{dn}{d\ln r_v} = \frac{1}{V(r_v)} \frac{df(\sigma, \delta_v)}{d\ln\sigma} \frac{d\ln\sigma^{-1}}{d\ln r_v},$$ (6)

where r_v is the late-time evolved radius of voids. A better agreement for the VSFs between simulations and the new model is achieved, after cleaning their simulated void catalogues to retain only non-overlapping voids (Jennings et al., 2013; Ronconi and Marulli, 2017; Ronconi et al., 2019).

Once the initial matter density power spectrum is specified, the abundance of voids can be predicted with the above equation. Note that the formation barrier of voids and the corresponding density contrast of the nonlinear void come necessarily from the spherical model, assuming a top-hat initial density. Having different initial density profiles will certainly lead to different formation barriers of voids, and different predictions for the VSF. Nonetheless, this model provides a useful guidance for the general physical picture of voids in the following aspects: the distribution of voids in terms of their sizes follows a Press-Schechter-type (Press and Schechter, 1974) function – large voids are rare compared to small ones.

Recently, by combining the excursion-set approach with the peak theory formalism in Lagrangian space, Verza et al. (2024) have succeeded in having a more accurate prediction for the void distribution function over a large range of scales (see Figure 3). This brings the application of the distribution function of voids for precise cosmological measurements a step closer.

The model is derived for the matter density field. When using tracers of dark matter, such as dark matter haloes or galaxies, to define voids, as is the case in real observations, Ronconi et al. (2019); Contarini et al. (2019) show that the model still works well, provided that the density contrast between the tracers versus dark matter is calibrated.

3.1 Applications

The VSF has been proposed as a means to test theories of gravity. For modified theories of gravity, in the standard excursion set theory, δ_v can depend on scale and environmental density (Clampitt et al., 2013; Voivodic et al., 2017). This leads to different VSFs compared to the VSF in general relativity. In coupled scalar field models for example, due to the 'screening mechanism', the strength of gravity may vary depending on the density environment. The dynamics of voids are particularly sensitive to it. This may lead to different abundances of voids in those models (Clampitt et al., 2013; Lam et al., 2015; Voivodic et al., 2017). Predictions for the VSFs from the $f(R)$ and symmetron models from N-body simulations by Cai et al. (2015); Voivodic et al. (2017) qualitatively confirm this, although, it was also shown that when mock galaxies are used to define voids, it becomes challenging to distinguish different models (Voivodic et al., 2017).

The sum of neutrino masses has been shown to leave its signature in the VSF. Using cosmological N-body simulations, Massara et al. (2015) shows that voids in massive neutrino cosmologies are less evolved than those without neutrinos: there is a larger number of small voids and a smaller number of large ones. Kreisch et al. (2019) shows that increasing the mass of the neutrinos increases the number of small dark matter voids and decreases the abundance of large voids. The opposite effect is found when using highly biased dark matter halos to define voids. The halo mass function in void environments is also found to be more sensitive to the sum of the masses of neutrinos (Zhang et al., 2020). Combining the VSF with the halo mass function and power spectrum can also help to tighten the constraints on the mass of neutrinos (Bayer et al., 2021). In observations, analyses with data from the SDSS-BOSS galaxy sample suggests that having void statistics adds modest but nonzero information beyond galaxy clustering. Void statistics may also be effective at constraining the sum of neutrino masses from below (Thiele et al., 2024). The VSF at high redshifts could also be useful to break the degeneracy between the sum of neutrino masses and the strength of gravity in the $f(R)$ model (Contarini et al., 2021).

In observations, Sahlén et al. (2016) used extreme-value statistics on the largest void from the 2MASS-WISE galaxy catalogue and cluster from the Atacama Cosmology Telescope (ACT) to constrain Ω_m and σ_8, the matter density parameter and the density dispersion of
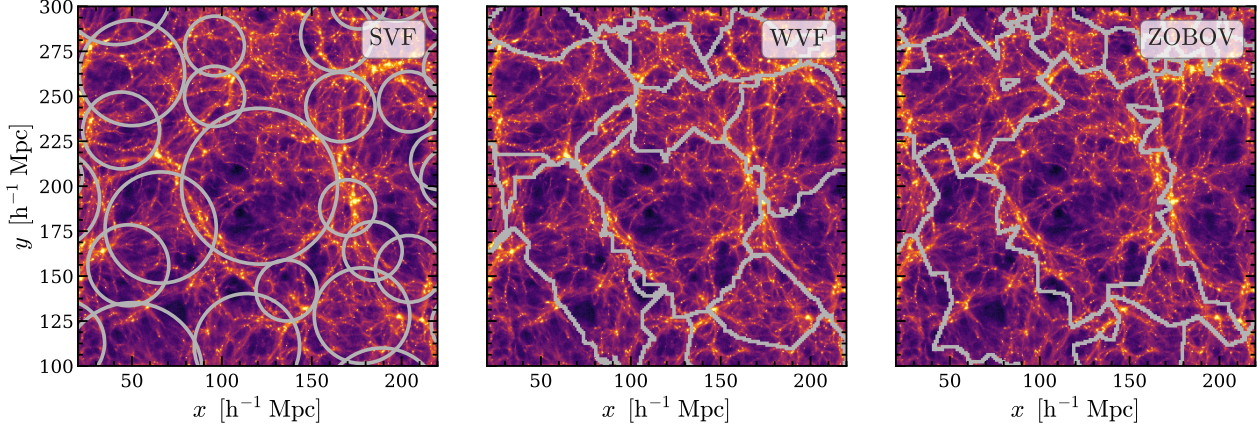
Fig. 6 Comparing three different void finding algorithms for voids identified in the same cosmological N-body simulation. The spherical void finder (SVF) (Padilla et al., 2005), the watershed void finder (WVF) (Platen et al., 2007) and the ZOBOV void finder (Neyrinck, 2008) are shown on the left, the middle and the right. Grey curves representing boundaries of voids are drawn on top of the projected density of dark matter. Despite some detailed differences for the exact borders of voids, the largest void regions in the simulation are consistently found by all the three algorithms. This figure is taken from Figure 2 of Paillas et al. (2019).

the linear-theory density field in 8 Mpc/h spheres. Contarini et al. (2023, 2024) used voids from the SDSS-BOSS-DR12 sample to obtain $\sim 10\%$ constraints in Ω_m, σ_8, and the parameter for the dark energy equation of state. They have also demonstrated that compared to the halo mass function, the VSF is sensitive to density perturbations on larger scales, they are therefore complementary to each other (Pelliciari et al., 2023). A similar level of precision for cosmological constraints was obtained using voids in the SDSS-DR7 sample (Fernández-García et al., 2024), fitted to the model developed in Betancort-Rijo et al. (2009).

Sahlén and Silk (2016) demonstrated that combining void abundance with cluster abundance can break degeneracies among cosmological parameters and offers constraints on modified gravity via the linear growth rate index γ from $f = \Omega_m^\gamma$. Sahlén (2019) further showed that the combination of VSF and halo mass function is able to break the degeneracy between the dark energy equation of state and the sum of neutrino masses. Using a simulation-based modelling framework, Thiele et al. (2024) has shown that the VSF adds modest extra constraints to the sum of neutrino mass. The constraint for the dark energy equation of state with Euclid has been predicted to be below 10% (Contarini et al., 2022). Percent-level constraints for cosmological parameters with the VSF from the CSST survey are expected (Song et al., 2024).

3.2 Finding voids in simulations and observations

In simulations and observations, individual voids have a wide variety of shapes, depths and density profiles. There is no clear definition for what should be called a void. It is unambiguous that they should be under-dense, but how to define their centres, where are their boundaries and how underdense should they be, are all somewhat uncertain. The flexibility of their definition has led to the development of a range of algorithms to find them. Figure 6 compares voids identified in the same simulation using three different void finding algorithms, the spherical void finder (Padilla et al., 2005), the watershed void finder (Platen et al., 2007) and ZOBOV (Neyrinck, 2008). We can see that the largest voids are found by all the three algorithms, but their boundaries and centres are all different. In addition, small voids found in one algorithm (SVF) may not be identified in another algorithm (ZOBOV). These differences indicate that the statistical properties of voids may depend on the void finding algorithm. The cosmological applications of them may need to account for this.

There are two main categories of void finding algorithms: underdensity-finding, and dynamical. The first uses the distribution of matter or tracers of matter to define under-dense regions, such as the spherical void finding algorithm (e.g. Hoyle and Vogeley, 2002; Padilla et al., 2005), watershed based algorithms (Colberg et al., 2005; Platen et al., 2007; Neyrinck, 2008) and the Popcorn void finding algorithm (Paz et al., 2023). The spherical void finder identifies regions of the Universe which satisfy a void density threshold, such as the one derived from the spherical evolution model $\delta_v = -0.8$. ZOBOV locates density depressions using a Voronoi tessellation to measure density at the location of each galaxy. From the lowest density depressions, a watershed algorithm is applied to group neighbouring Voronoi cells into 'zones' to form voids (Neyrinck, 2008).

The second category uses dynamical quantities such as the velocity divergence and phenomena such as stream-crossing to identify voids. For example, with the Hessian matrix of the smoothed density field, or the gravitational potential field, one can identify voids as regions with all three eigenvalues below a certain threshold (e.g. Hahn et al., 2007; Forero-Romero et al., 2009; Lavaux and Wandelt, 2010; Aragón-Calvo et al., 2010; Hoffman et al., 2012; Cautun et al., 2014). The scale of smoothing and the thresholds for the eigenvalues are free parameters in these algorithms. Some dynamical methods are arguably physically objective, but rely on information available only in simulations, not straightforwardly in observations. Shandarin et al. (2012) combined information of density and velocity i.e., the full 6D phase space information to classify the cosmic web, including voids. Falck et al. (2012) classified particles in simulations as 'void' particles if they undergo no crossings with respect to any other particles over the course of a simulation. In some cases, the void particles may not be easily separable into idealized, nearly convex or polyhedral shapes, but instead may be better thought of a void region that percolates
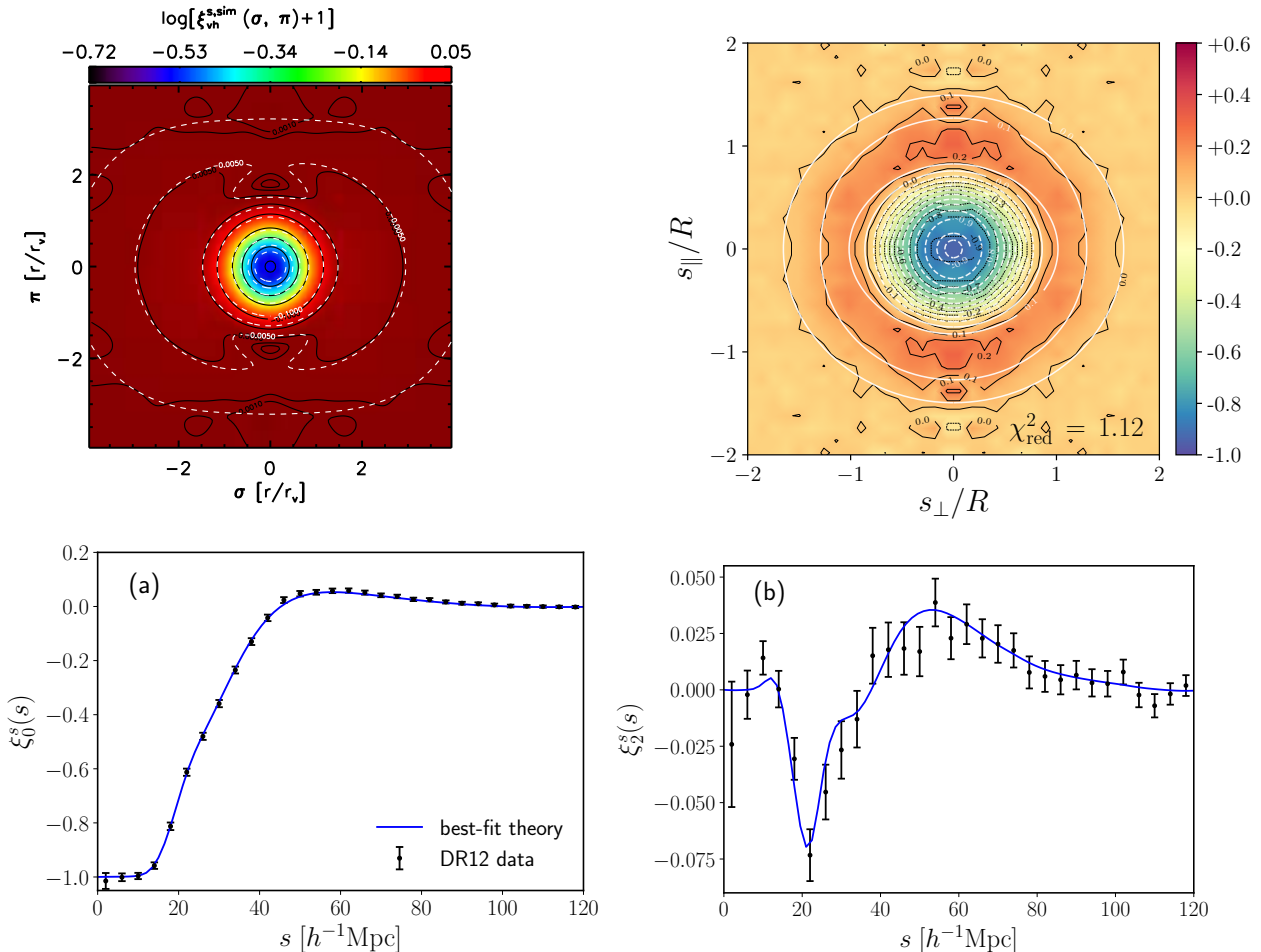
Fig. 7 Top-left: comparing the void-halo correlation function in redshift space measured from simulations with linear theory. The black contours are results from the simulation, and the white contours are the best-fit linear model (Cai et al., 2016). Top-right: void-galaxy correlation function measured from the SDSS-BOSS-DR12 galaxy sample. The black contours are results from observation, and the white contours are the best-fit model from linear theory. The inverse Abel transformation was used for reconstructing the real-space void-galaxy correlation function (Hamaus et al., 2020). Bottom-left and bottom-right: the monopole and quadrupole moments of the void-galaxy correlation function measured with the SDSS-BOSS-DR12-CMASS galaxy sample. Data points with errors are from observations; the blue lines are the best-fit model based on the Gaussian streaming model. Reconstruction with the Zeldovich approximation was used to recover the real-space void-galaxy correlation function (Nadathur et al., 2020). From fitting to the measurements, a few percent-level constraints for the growth parameter and the AP parameters have been achieved (Hamaus et al., 2020; Nadathur et al., 2020). These plots are taken from the above three papers mentioned.

wherever galaxies, filaments and walls are not (Falck et al., 2015; Stücker et al., 2018)

In general, the characteristic of voids being under-dense converges among different algorithms, but the quantitative measurement for the abundance of voids as a function of radius may differ significantly. Which algorithm to choose may depend on the specific application for cosmology or astrophysics. A summary comparing different algorithms can be found in Colberg et al. (2008) and also in Libeskind et al. (2018) in the context of the cosmic web.

In observations, samples of voids have been identified in major galaxy redshift surveys and lensing surveys. These include voids in the CfA survey (Vogeley et al., 1991), the Point Source Catalog redshift (PSCz) survey (Hoyle and Vogeley, 2002), the Two-Degree Field Galaxy Redshift Survey (Hoyle and Vogeley, 2004), and the Dark Energy Survey (DES) (Sánchez et al., 2017; Kovács et al., 2022c). Perhaps the most exploited dataset for voids is in the SDSS area (Pan et al., 2012; Sutter et al., 2012; Cai et al., 2014; Nadathur, 2016; Mao et al., 2017; Zhao et al., 2020, 2022; Douglass et al., 2023; Tamone et al., 2023). These have been used to constrain cosmological parameters via redshift-space distortions (Kaiser, 1987) and the Alcock-Paczyński (AP) effect (Alcock and Paczynski, 1979), measure the growth of structure, constrain the sum of neutrino masses via the effect of gravitational lensing, and study the imprints of voids on the CMB via the integrated Sachs-Wolfe (ISW) effect (Sachs and Wolfe, 1967).

4 Redshift-space distortions around voids

Galaxy redshift surveys such as SDSS and DESI (DESI Collaboration et al., 2016) provide the 3D distribution of millions of galaxies over a large volume of the Universe. Voids can be identified in these surveys from finding under densities in the galaxy number density field, which is thought to be tracing the underlying large-scale structure of matter. Stacking the galaxies number densities around void centres yields the void-galaxy correlation function $\xi_{vg}(s_\perp, s_\parallel)$, where $s_\perp$ and $s_\parallel$ are the redshift-space transverse and line-of-sight distances from the centre of the voids. When averaging over a large sample of voids, the real-space void-galaxy correlation function $\xi_{vg}(r)$ should be isotropic, but $\xi_{vg}(s_\perp, s_\parallel)$ is anisotropic due to (i) redshift-space distortions (Kaiser, 1987), and (ii) the Alcock-Paczynski (AP) effect (Alcock and Paczynski, 1979). The joint analyses of these two effects with the observed void-galaxy correlation function provides complementary constraints for cosmological parameters. It has emerged as a major cosmological probe.

4.1 Dynamical distortions

The effect of redshift-space distortions arises from the fact that the observed line-of-sight distance of a galaxy $s_\parallel$ is perturbed by its peculiar velocity $v_\parallel^{\mathrm{pec}}$ along the line of sight

$$s_\parallel = r_\parallel + v_\parallel^{\mathrm{pec}}/[aH(a)], \tag{7}$$

where $r_\parallel$ is the real-space comoving distances of a galaxy, a is the scale factor of the Universe and $H(a)$ is the Hubble parameter at a. This effect leads to dynamical distortions for the observed void-galaxy correlation function. The distortion is small, but is detectable with a large sample of voids.

The mapping between the redshift-space void-galaxy correlation function $\xi_{vg}(s_\perp, s_\parallel)$ and its real-space counterpart $\xi_{vg}(r)$ encodes information about peculiar velocities. To extract cosmological information from this measurement, we need a model to connect them. The number of galaxies around voids is conserved in the mapping from real to redshift space. With the plane-parallel approximation where $v_\parallel^{\mathrm{pec}}/[aH(a)] \ll 1$, keeping all terms to the linear order, $\xi_{vg}(r) \ll 1$ and $\partial v(r)/\partial r \ll aH(a)$ (Cai et al., 2016),

$$\xi_{vg}(s_\perp, s_\parallel) = \xi^r(r) + \frac{1}{3}\beta\bar{\xi}^r(r) + \beta\mu^2[\xi^r(r) - \bar{\xi}^r(r)], \tag{8}$$

where $\mu = \cos\theta$ and θ is the subtended angle from the line of sight; $\beta = f/b$ and $f = d\ln D/d\ln a$ is the linear growth rate with D being the linear growth factor and b is the linear galaxy bias, a factor of proportionality between the amplitude of clustering in galaxies and matter. $\bar{\xi}^r(r) = \frac{3}{r^3}\int_0^r \xi^r(r')r'^2 dr'$ is the volume averaged real space void-galaxy correlation function. Note that $\xi_{vg}(r)$ is the real-space density profile of voids traced out by galaxies. In linear theory, $\xi_{vg}(r) = b\delta(r)$, and so $\bar{\xi}^r(r)$ is coupled to the peculiar velocity via Equation 3. An example of the model and its comparison with measurements from simulations and observations is shown in the top panels of Figure 7. The model thus encodes information about the peculiar velocity, which is related to the growth parameter β. This enables us to constrain the growth parameter.

Linear theory applies to regions where the density fluctuation is small. This is a good approximation on large scales, but it may not be the case near the centre of voids. For the more general cases, the streaming model (Peebles, 1980) is exact:

$$1 + \xi_{vg}(s_\perp, s_\parallel) = \int [1 + \xi^r(r)]p(r, v_\parallel^{pec})dv_\parallel^{pec}, \tag{9}$$

but it requires knowing the real-space correlation function and the full velocity distribution function $p(r, v_\parallel^{pec})$ (Peebles, 1980; Paillas et al., 2021), which is challenging. By assuming that the velocity distribution function is Gaussian, the above equation becomes

$$1 + \xi_{vg}(s_\perp, s_\parallel) = \int [1 + \xi^r(r)]\frac{1}{\sqrt{2\pi\sigma_v^2(r,\mu)}}\exp\left[-\frac{v_\parallel - v^{pec}(r)\mu}{2\sigma_v^2(r,\mu)}\right]dv_\parallel^{pec}, \tag{10}$$

where $v^{pec}(r)$ is the radial peculiar velocity profile, and $\sigma_v^2(r,\mu)$ is the velocity dispersion. This is the so-called Gaussian streaming model (Fisher, 1995). It was shown to be more accurate than the linear one down to relatively small scales (Paz et al., 2013; Hamaus et al., 2015; Cai et al., 2016; Nadathur, 2016; Nadathur and Percival, 2017; Paillas et al., 2021).

4.2 Geometric distortions

In addition to the dynamical distortion, geometric distortions around voids arise when converting the observed redshifts of galaxies into distances (Lavaux and Wandelt, 2012; Hamaus et al., 2014a). To do so, we need to assume a fiducial cosmological model to have the distance-redshift relationship. If the fiducial model is different from the true underlying cosmology of the Universe, all the distances will be stretched, an effect known as Alcock-Paczynski (AP) distortions (Alcock and Paczynski, 1979). The AP effect amounts to a universal re-scaling for the line-of-sight and transverse distances compared to the fiducial cosmology (Ballinger et al., 1996): $s_\perp = q_\perp s'_\perp$ & $s_\parallel = q_\parallel s'_\parallel$, where the prime represent quantities in the fiducial cosmology. The two scaling factors are related to cosmological parameters via $q_\perp = D_M/D'_M$ and $q_\parallel = H/H'$ where D_M is the angular diameter distance and H is the Hubble parameter.

The AP effect enters the observed void-galaxy correlation function (e.g. Equation 8) through coordinate transformations: $\xi^s(s_\perp, s_\parallel) = \xi^s(q_\perp s'_\perp, q_\parallel s'_\parallel)$. It interferes with the interpretations of the dynamical distortion, but the two effects are not degenerate. In cosmological parameter inferences, both effects will be modelled in $\xi^s(s_\perp, s_\parallel)$. This enables us to constrain cosmological parameters by comparing the model against observations. Examples of this kind of analysis are shown in Figure 7.
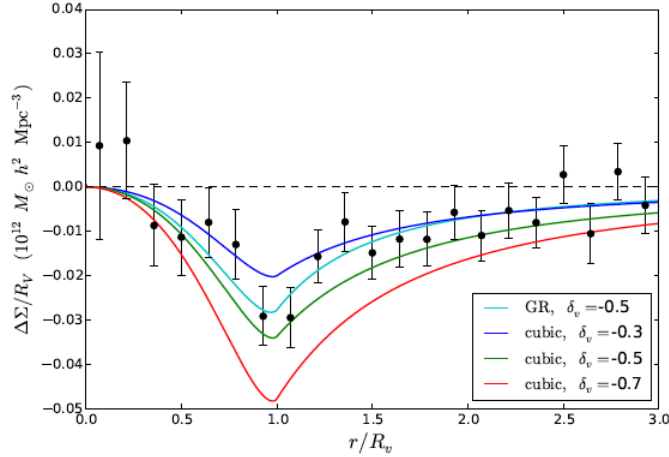
Fig. 8 Comparing the observed lensing tangential shear profiles (data points with errors) around SDSS voids using the SDSS LRG galaxy image data with different models. Coloured lines are model predictions from general relativity and the Cubic Galileon model with different central densities of voids, as indicated by the legend. The profiles are normalised by the radius of each void, as indicated in the x-axis. The figure is taken from Figure 3 of (Baker et al., 2018).

4.3 Applications

Redshift-space distortions around voids encode information about the density and velocity. This is ideal for capturing the difference between general relativity and non-standard gravity models, where violation of the equivalence principle may occur most evidently in voids. Therefore, redshift-space distortions around voids is a promising observable which can capture the combination of these two effects (Cai et al., 2015, 2016). Recent tests with mock catalogues confirm the physical scenario, but find that at the statistical precision offered by a volume of ~ 1 $(Gpc/h)^3$, the linear growth parameter fitted from redshift-space distortions can not distinguish between general relativity and their specific choice of the $f(R)$ and nDGP models (Wilson and Bean, 2023). Mauland et al. (2023) used the void-galaxy correlation function to investigate the degeneracy between massive neutrinos and $f(R)$ modified gravity, but concluded that at the accuracy of a few percent, the present modelling is insufficiently accurate to do so.

In observations, analyses of redshift-space distortions around voids to constrain the growth rate parameter have been reported in Achitouv et al. (2017) from the 6dF Galaxy Survey, and Hawken et al. (2017) from the VIPERS survey, delivering constraints for the growth parameter on the order of $\sim 10\%$. The joint analysis of redshift-space distortions and the AP distortions has emerged to become a major cosmological probe. It has been applied to data from the SDSS-BOSS and eBOSS surveys from multiple research groups with different methods (Hamaus et al., 2016, 2017; Achitouv, 2019; Nadathur et al., 2019b; Hamaus et al., 2020; Hawken et al., 2020; Nadathur et al., 2020; Aubert et al., 2022; Woodfinden et al., 2022, 2023; Fraser et al., 2024). Despite the differences in the choice of modelling among different research teams, most of them are able to bring down the constraints on the growth parameter to a few percents level (see Figure 7 for results from different analyses of a similar dataset.). This is complementary and comparable to the standard two-point statistics. This may indicate that like other conventional analyses of large-scale structure, the RSD and AP analyses around voids are already limited by systematic errors, including observational systematics and limitations in the accuracy of our modelling.

A common underlying assumption for all the above models of redshift-space distortions is that the centres of voids do not move. This is not exactly the case. Void centres do have peculiar velocities, and this complicates the modelling of redshift-space distortions (Chuang et al., 2017; Nadathur et al., 2019a). In addition, Correa et al. (2022) points out the void-galaxy correlation may also be complicated by the ellipticity of voids. Two approaches have been developed to deal with this, by reconstructing the real-space void-galaxy correlation function from data itself. Hamaus et al. (2020) deproject the observed projected correlation void-galaxy correlation function; Nadathur et al. (2019a) proposes using velocity reconstructions to remove redshift-space distortions. Both have been demonstrated to deliver unbiased constraints for cosmological parameters with mock catalogues, and have set some of the tightest constraints for the growth parameters with data from BOSS (Hamaus et al., 2020; Nadathur et al., 2020). They have also been predicted to deliver percent-level constraints for the growth parameter and sub-percent-level constraints for the AP parameters with Euclid (Hamaus et al., 2022; Radinović et al., 2023).

It is also worth mentioning that the void-void clustering, together with the void-galaxy clustering has been shown to provide extra information about the baryon acoustic oscillations (BAO), these have helped to tighten the constraints for the AP parameters (Kitaura et al., 2016; Liang et al., 2016; Zhao et al., 2020, 2022; Tamone et al., 2023).

5 Gravitational lensing by voids

Cosmic voids can be substantial gravitational potential hills, which generally deflect photons passing through them. The spatial and temporal variations of the metric gravitational potentials $\Phi(x,t) + \Psi(x,t)$ generates observational effects on photons. The spatial gradients in $\Phi + \Psi$
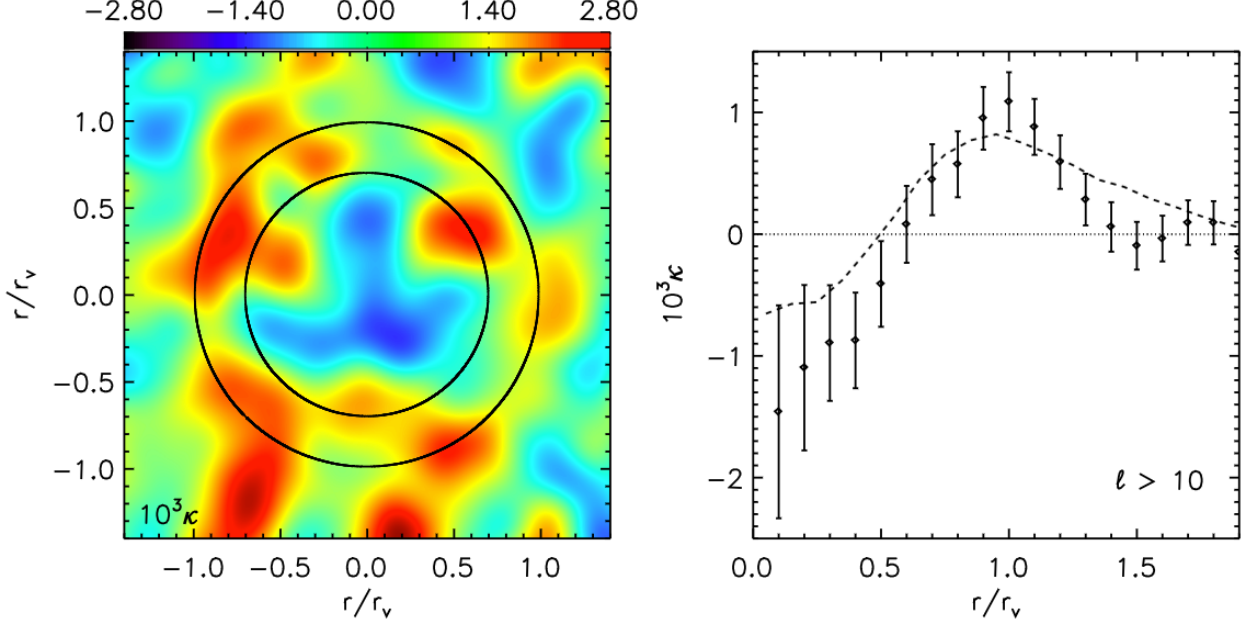
Fig. 9 Left: the stacked map of CMB lensing convergence κ from Planck (Planck Collaboration et al., 2014) with the locations of voids found in the SDSS-BOSS-DR12-CMASS galaxy sample. Voids with the radius $r_v > 20$ Mpc/h are used for the stacking. The inner circle of radius and equal-area outer ring mark the extent of the compensated filter, normalised with r_v. Right: the averaged convergences from the centre of the stacking on the left. Data points with errors are measurements from observations; the dashed line is the measurement from mock catalogues from the standard ΛCDM model, which agrees with the observational data within the errors (Cai et al., 2017). The figure is taken from Figure 3 of Cai et al. (2017).

give rise to the gravitational lensing effect around voids, which is characterised by the lensing potential:

$$\psi_{\text{lens}} = \frac{1}{c^2} \int \frac{D_{ls}}{D_s D_l} (\Phi + \Psi) dz, \tag{11}$$

with Φ and Ψ being respectively the time and space parts of the metric potentials in the perturbed FRLW metric. ψ_{lens} is defined as the lensing potential, z is the redshift, and D_l, D_s and D_{ls} are the line-of-sight angular diameter distances of the lens, the source and that between the lens and the source, respectively.

The 2D Laplacian of the lensing potential is related to the lensing convergence κ via $\kappa = \frac{1}{2}\nabla^2 \psi_{\text{lens}}$. In general relativity where $\Phi = \Psi$, it can be expressed as

$$\kappa = \frac{3H_0^2 \Omega_m}{2c^2} \int \frac{D_l D_{ls}}{D_s} \frac{\delta}{a} dz. \tag{12}$$

The lensing convergence is therefore related to the projected mass density contrast δ along the line of sight. Gravitational lensing by voids therefore provides a means to measure the projected mass distribution around voids.

The gravitational lensing by voids affects any light shining from behind the voids, from the cosmic microwave background and galaxies. The effect can be detected by observing the coherent distortions of the CMB temperature map, called CMB lensing; or the coherent shear signal on the images of background galaxies, which may be called void-galaxy lensing.

Cross-correlations between voids with a reconstructed map of the lensing convergence, either coming from the CMB, or from the surveys of galaxy images, offers a direct way to measure the projected mass density around voids. Alternatively, the projected density profiles of voids can be measured by directly stacking the shear signal of the background galaxies around them. The lensing convergence profile is related to the tangential component of the shear γ_t via,

$$\gamma_t(R_p) = \kappa(< R_p) - \kappa(R_p), \tag{13}$$

where $\kappa(R_p)$ and $\kappa(< R_p)$ are the average convergence at the projected radius R_p and within R_p from the void centre. Figure 8 shows an example of the lensing tangential shear profiles around voids measured from the SDSS LRG galaxy sample. Figure 9 shows the first detection of the CMB lensing convergence around voids from the SDSS-CMASS sample.

A prediction for lensing by individual voids was made in Amendola et al. (1999), concluding that only voids with radius greater than 100Mpc/h will have the signal-to-noise ratio of unity. The first forecasts for the detectability of void lensing via stacking was made by

Krause et al. (Krause et al., 2013) and Higuchi et al. (Higuchi et al., 2013). Detections of the signal from lensing surveys were first made in the SDSS area (Melchior et al., 2014; Clampitt and Jain, 2015), and later with the DES science verification data (Gruen et al., 2016; Sánchez et al., 2017) and year-1 data (Fang et al., 2019; Vielzeuf et al., 2021), and at high redshifts with the Lyman$-\alpha$ forest tomography in the COSMOS field (Krolewski et al., 2018), and in more recent data releases of the DES survey.

CMB lensing of voids has been detected by stacking the reconstructed lensing convergence from CMB lensing, first in the SDSS area (Cai et al., 2017; Chantavat et al., 2017; Raghunathan et al., 2020). Detections have been made using the cross-correlations of other major galaxy surveys: the WISE-Pan-STARSS data set (Camacho-Ciurana et al., 2023), the DES area (Kovács et al., 2022c; Demirbozan et al., 2024) and the DESI legacy survey data (Hang et al., 2021; Dong et al., 2021b). The signal-to-noise ratio of lensing by voids is now sufficiently significant that it has been used to constrain the amplitude parameter of lensing convergence A_κ, as a consistency check between the linear growth parameter and the effect of gravitational lensing.

5.1 Applications

Gravitational lensing by voids is a major way to measure the total matter density profile of voids. Despite the line-of-sight projection effect, which erases some information from the full 3D voids, most cosmological applications of individual voids mentioned in Section 2 rely on the measurements of lensing. The effect is therefore expected to be powerful for constraining the sum of neutrino masses and testing theories of gravity.

Neutrinos have a higher mass fraction in voids, since they are diffuse compared to other matter. So, the impact of neutrinos on the growth of structure is expected to be stronger in voids than in high-density regions. Forecasts with simulations have shown that the profiles of voids are indeed a sensitive probe of neutrino masses (e.g. Massara et al., 2015; Coulton et al., 2020), and that gravitational lensing by voids has the potential to set constraints on the sum of neutrino masses (e.g. Vielzeuf et al., 2023). Forecasts for the Euclid survey also indicate that lensing of voids can provide better constraints on other cosmological parameters when combined with other cosmological probes (Bonici et al., 2023).

For theories of gravity with coupling between the strength of gravity and matter density, the density profiles of voids will be altered compared to their version in standard gravity. This can be detected through lensing of voids (Clampitt et al., 2013; Cai et al., 2015; Cautun et al., 2018; Davies et al., 2019). For others, such as the Galileon models (or the massive gravity model), the relation between the lensing potential and the density perturbation can be modified. The lensing signal around voids can be very different, even with the same mass density as in general relativity. Lensing of voids can therefore be used to distinguish them from general relativity (Barreira et al., 2015; Baker et al., 2018; Su et al., 2023). An example of this kind is given in Figure 8. When combined with the two-point correlation function, lensing of voids is also useful to break the degeneracy among cosmological parameters (Davies et al., 2021). In addition, the effect of gravitational lensing probes the sum of the two metric potentials, the motions of galaxies respond only to the Newtonian potential. The combination of lensing and redshift-space distortions can be used to test the gravitational slip (e.g. Zhang et al., 2007; Reyes et al., 2010; Alam et al., 2017; Amon et al., 2018; Singh et al., 2018; Skara and Perivolaropoulos, 2020; Wenzl et al., 2024). This applies to voids, where the gravitational slip, if any, may be stronger (Spolyar et al., 2013).

An extended version of lensing around voids is 'troughs', which measures the lensing signal around under densities in 2D projected galaxy number density fields (Gruen et al., 2016; Barreira et al., 2017; Friedrich et al., 2018; Gruen et al., 2018; Brouwer et al., 2018). An analytical model to predict the signal has been developed in Gruen et al. (2016); Friedrich et al. (2018), which allows for constraints on cosmological parameters. The method has been applied to data from the Dark Energy Survey (Gruen et al., 2016, 2018), and the Kilo-Degree Survey (Burger et al., 2023), delivering complimentary and comparable constraints on Ω_m-σ_8 and the galaxy bias parameter b compared to the conventional lensing 3×2 analyses of the same data.

6 The imprints of voids on the cosmic microwave background

The spatial perturbation of the gravitational potentials by voids causes gravitational lensing effects of the CMB, as discussed in the previous section. The temporal perturbation of the potentials induced by voids alters the energy of photons traversing them. This induces additional temperature fluctuations of the CMB, known as the Integrated Sachs-Wolfe (ISW) effect (Sachs and Wolfe, 1967):

$$\frac{\Delta T}{T_{\text{CMB}}} = -\frac{1}{c^2} \int (\dot{\Phi} + \dot{\Psi}) dt, \tag{14}$$

where the $\dot{\Phi}$ and $\dot{\Psi}$ are the time derivative of the metric potentials and T_{CMB} is the CMB temperature. In a ΛCDM universe, the accelerating expansion of the Universe caused by dark energy stretches cosmic voids and superclusters, causing their gravitational potentials to decay. CMB photons travelling through them will lose/gain energy. The observed CMB temperature along the line of sight of a void/supercluster will decrease/increase by the amount specified by Equation 14. A detection of the ISW signal can therefore provide constraints on dark energy. It can also be used to constrain theories of gravity (Song et al., 2007; Lombriser et al., 2012; Barreira et al., 2014; Renk et al., 2017).

In the standard ΛCDM model, the ISW signal is much smaller than the primordial CMB temperature fluctuation. This is a challenge for its direct detection. One way to detect the signal is by stacking the CMB temperature map with voids and superclusters found in galaxy redshift surveys. This should yield a cold and hot spot respectively for voids and superclusters. It was first conducted in Granett et al. (2008) where a somewhat unexpected high significance ($\sim 4\sigma$) result was reported by stacking superstructures found from the photo-z galaxy catalogue in the SDSS area (see Figure 10 for the main results). However, the amplitudes of the signal were higher than expected
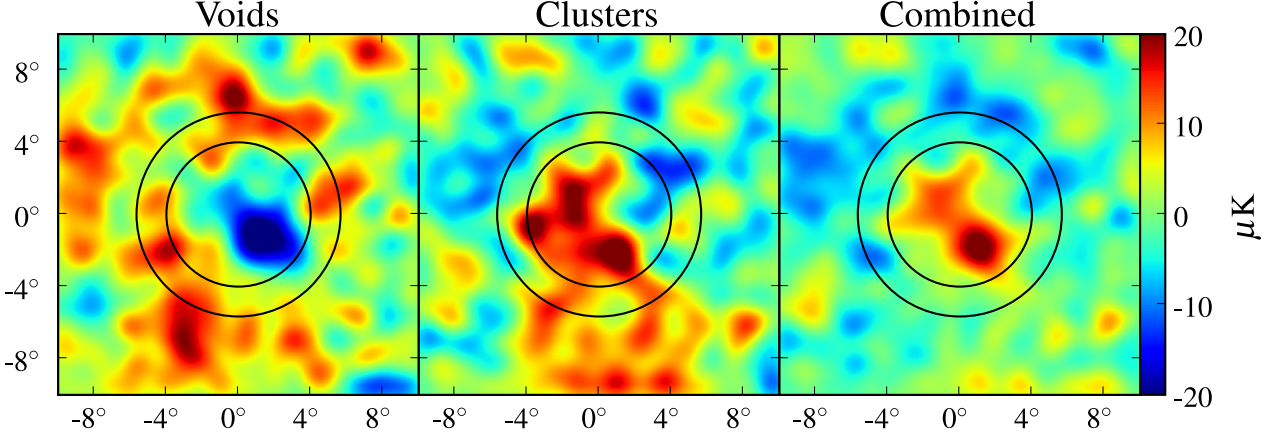
Fig. 10 Stacked regions on the temperature map of the CMB corresponding to 50 voids and 50 superclusters identified in the SDSS Luminous Red Galaxy (LRG) sample. Cold and hot spots appear in the void and cluster stacks, respectively, with a characteristic radius of four degrees, corresponding to the scale of 100 Mpc/h. The sign of the signal from voids is flipped and averaged with the signal from the superclusters, shown as 'Combined'. These are expected if dark energy is causing the gravitational potentials of voids and superclusters to decay – the observation can be taken as a piece of evidence of dark energy. However, the amplitude of the signal, which is at the order of 10 μK, is a few times higher than expected in the standard ΛCDM model (Granett et al., 2008). The figure is taken from Figure 1 of Granett et al. (2008).

from the standard ΛCDM model. Follow-up analysis using similar methods with spectroscopic redshift catalogues (but still in the SDSS area) confirms the results qualitatively (Nadathur et al., 2012; Flender et al., 2013; Ilić et al., 2013; Cai et al., 2014; Kovács and Granett, 2015; Planck Collaboration et al., 2016; Aiola et al., 2015; Cai et al., 2017; Kovács, 2018; Kovács et al., 2019, 2022a), which may indicate a tension with the standard model, but agreement with the standard model was found in Nadathur and Crittenden (2016) when a matched filter approach was used in the analysis. Using a larger survey area from the DESI legacy survey Hang et al. (2021); Dong et al. (2021a,b) also do not find evidence of an excess ISW signal around voids and superclusters. It has also been argued that through the ISW effect, the Eridanus Supervoid (Szapudi et al., 2015) contributes substantially (or modestly; see Kovács et al. (2022b)) to the somewhat anomalous temperature decrement in the Cold Spot (Cruz et al., 2005), a several-degree patch on the CMB.

While the amplitudes of the ISW signal around voids and superclusters may still be debatable among different studies, all the above analyses have found the sign of the signal to be consistent with expectation from the standard model. These results, together with the positive cross-correlation between the galaxy samples with the CMB, indicate that the late-time gravitational potentials are indeed decaying. This has placed strong constraints on the Galileon model (Renk et al., 2017).

Both the effects of CMB lensing and ISW are gravitational interactions between voids and CMB photons. Other astrophysical processes, such as the thermal Sunyaev-Zel'dovich effect (Sunyaev and Zeldovich, 1970, 1980a) (tSZ) also occur between voids and the CMB.

The tSZ effect arises from inverse Compton scattering of free electrons to CMB photons, inducing additional fluctuations for the observed CMB temperature (Sunyaev and Zeldovich, 1970):

$$\frac{\Delta T}{T_{\mathrm{CMB}}} \propto \int n_e T_e d\ell, \tag{15}$$

where n_e and T_e are the electron number density and temperature. $d\ell$ integrates along the line of sight between the observer to the CMB. The tSZ effect can be used to measure the projected electron pressure $n_e T_e$ around voids. With additional information about the gas temperature T_e, the abundance of baryons, which can be approximated by the number density of free electrons, can be constrained. Detections of the tSZ effect around voids have been reported in Alonso et al. (2018); Li et al. (2024). Measurements of the baryon content in voids, compared with the baryon fractions in other types of the cosmic web: galaxy clusters, filaments and walls, may be able to help to understand the baryon cycle in the Universe.

7 The impact of a local void on the perception of cosmic expansion

One intriguing hypothesis is that the observed late-time acceleration of the Universe could be explained by our position near the center of a large, shallow void perhaps hundreds of Mpc across. This would arguably be large enough to challenge the cosmological principle (that we live in a typical region of the Universe). The density of the void increases with the radial distance R from the observer. Eventually, at sufficiently large R, the average density of the void approaches the mean density of the Universe. Observers within this void would perceive a locally faster expansion rate compared to a homogeneously matter-dominated Universe. As R increases and the density contrast diminishes,

the observed expansion rate would increasingly resemble that of a standard matter-dominated Universe. By adjusting the density profile of such a void, it is possible to mimic the observed accelerated expansion history of the Universe in a matter-dominated universe without dark energy (e.g. Barausse et al., 2005; Alnes et al., 2006; Garcia-Bellido and Haugbølle, 2008).

However, the hypothesis was largely ruled out by observations of the kinetic Sunyaev-Zeldovich (kSZ) effect (Sunyaev and Zeldovich, 1980a,b), which measures the peculiar velocities of galaxy clusters through the CMB rest frame. If the local void is large and deep enough to explain dark energy, we would expect a much larger kSZ effect than we have actually observed. The observed kSZ effect is in fact consistent with the predictions of the ΛCDM model and this places stringent constraints on large-scale inhomogeneities, effectively disfavoring the void model as a primary explanation for cosmic acceleration (Zhang and Stebbins, 2011).

There is, however, observational evidence that our nearby environment is slightly underdense. Observations of galaxy number counts and the luminosity function suggest a local underdensity (e.g. Keenan et al., 2013; Whitbourn and Shanks, 2014), which could lead to the perception that the local Universe is expanding slightly faster than elsewhere. However, it is disputed whether this is sufficient to fully explain the Hubble tension – the apparently larger value of the Hubble constant measured locally compared to that inferred from CMB observations in the ΛCDM model (e.g. Shanks et al., 2019; Kenworthy et al., 2019; Mazurenko et al., 2025).

This local void is not to be confused with the Local Void, which has been clearly mapped. The Local Sheet, a cosmic wall in which the Milky Way is embedded, forms a boundary of the Local Void, a perhaps remarkably (Peebles and Nusser, 2010) deep void some 60 Mpc across (Tully and Fisher, 1987; Tully et al., 2019).

8 Summary

Cosmic voids as part of the cosmic web are some of the largest-scale structures of our Universe. The low-density nature of voids makes them unique in preserving the initial conditions of the Universe, and having arguably more direct sensitivity to the global expansion of the Universe. Analysing the large-scale structure from the perspective of cosmic voids can often provide us with new and complementary information about cosmology and astrophysics. They are useful in constraining cosmological parameters including dark energy, measuring the sum of neutrino masses and testing theories of gravity.

As a cosmological probe, cosmic voids have now been established as one of the beyond-two-point statistics. When combined with the conventional two-point statistics, they can often provide extra cosmological information. In the era of precision cosmology where systematic errors are dominating our measurements, this is both valuable and challenging. The reduction of statistical errors brought by extra probes from voids is likely to increase the requirement for the control of observational and theoretical systematics. Next generation galaxy surveys such as the ongoing surveys of DESI, LSST and Euclid promise to increase the current survey volume and number of galaxies by an order of magnitude. This offers great opportunities for advancing our understanding of cosmology using multiple cosmological probes. However, calibration of observational systematics is likely to remain the major challenge. Perhaps more valuable is to analyse the data independently, from the perspective of only cosmic voids. Being different from the conventional analyses, this may help to provide diagnostics for observational systematics.

Acknowledgments

See Also: Cosmic web

References

Achitouv I (2019), Dec. New constraints on the linear growth rate using cosmic voids in the SDSS DR12 datasets. *Phys. Rev. D* 100 (12), 123513. doi:10.1103/PhysRevD.100.123513. 1903.05645.

Achitouv I, Blake C, Carter P, Koda J and Beutler F (2017), Apr. Consistency of the growth rate in different environments with the 6-degree Field Galaxy Survey: Measurement of the void-galaxy and galaxy-galaxy correlation functions. *Phys. Rev. D* 95 (8), 083502. doi:10.1103/PhysRevD.95.083502. 1606.03092.

Aiola S, Kosowsky A and Wang B (2015), Feb. Gaussian approximation of peak values in the integrated Sachs-Wolfe effect. *PRD* 91 (4), 043510. doi:10.1103/PhysRevD.91.043510. 1410.6138.

Alam S, Miyatake H, More S, Ho S and Mandelbaum R (2017), Mar. Testing gravity on large scales by combining weak lensing with galaxy clustering using CFHTLenS and BOSS CMASS. *MNRAS* 465: 4853–4865. doi:10.1093/mnras/stw3056. 1610.09410.

Albrecht A and Steinhardt PJ (1982), Apr. Cosmology for Grand Unified Theories with Radiatively Induced Symmetry Breaking. *Phys. Rev. Lett.* 48 (17): 1220–1223. doi:10.1103/PhysRevLett.48.1220.

Alcock C and Paczynski B (1979), Oct. An evolution free test for non-zero cosmological constant. *Nature* 281: 358. doi:10.1038/281358a0.

Alnes H, Amarzguioui M and Grøn Ø (2006), Apr. Inhomogeneous alternative to dark energy? *Phys. Rev. D* 73 (8), 083519. doi:10.1103/PhysRevD.73.083519. astro-ph/0512006.

Alonso D, Hill JC, Hložek R and Spergel DN (2018), Mar. Measurement of the thermal Sunyaev-Zel'dovich effect around cosmic voids. *Phys. Rev. D* 97 (6), 063514. doi:10.1103/PhysRevD.97.063514. 1709.01489.

Amendola L, Frieman JA and Waga I (1999), Oct. Weak gravitational lensing by voids. *MNRAS* 309 (2): 465–473. doi:10.1046/j.1365-8711.1999.02841.x. astro-ph/9811458.

Amon A, Blake C, Heymans C, Leonard CD, Asgari M, Bilicki M, Choi A, Erben T, Glazebrook K, Harnois-Déraps J, Hildebrandt H, Hoekstra H, Joachimi B, Joudaki S, Kuijken K, Lidman C, Loveday J, Parkinson D, Valentijn EA and Wolf C (2018), Sep. KiDS+2dFLenS+GAMA: testing the cosmological model with the E_G statistic. *MNRAS* 479 (3): 3422–3437. doi:10.1093/mnras/sty1624. 1711.10999.

Aragon-Calvo MA (2023), Jun. Scaling relations in the network of voids. *MNRAS* 522 (1): L46–L50. doi:10.1093/mnrasl/slad037.

Aragon-Calvo MA and Szalay AS (2013), Feb. The hierarchical structure and dynamics of voids. *MNRAS* 428 (4): 3409–3424. doi:10.1093/mnras/sts281. 1203.0248.

Aragón-Calvo MA, van de Weygaert R and Jones BJT (2010), Nov. Multiscale phenomenology of the cosmic web. *MNRAS* 408 (4): 2163–2187. doi:10.1111/j.1365-2966.2010.17263.x. 1007.0742.

Aubert M, Cousinou MC, Escoffier S, Hawken AJ, Nadathur S, Alam S, Bautista J, Burtin E, Chuang CH, de la Macorra A, de Mattia A, Gil-Marín H, Hou J, Jullo E, Kneib JP, Neveux R, Rossi G, Schneider D, Smith A, Tamone A, Vargas Magaña M and Zhao C (2022), Jun. The completed SDSS-IV extended Baryon Oscillation Spectroscopic Survey: growth rate of structure measurement from cosmic voids. *MNRAS* 513 (1): 186–203. doi:10.1093/mnras/stac828. 2007.09013.

Baker T, Clampitt J, Jain B and Trodden M (2018), Jul. Void lensing as a test of gravity. *Phys. Rev. D* 98 (2), 023511. doi:10.1103/PhysRevD.98.023511. 1803.07533.

Ballinger WE, Peacock JA and Heavens AF (1996), Oct. Measuring the cosmological constant with redshift surveys. *MNRAS* 282: 877. doi:10.1093/mnras/282.3.877. astro-ph/9605017.

Barausse E, Matarrese S and Riotto A (2005), Mar. Effect of inhomogeneities on the luminosity distance-redshift relation: Is dark energy necessary in a perturbed universe? *Phys. Rev. D* 71 (6), 063537. doi:10.1103/PhysRevD.71.063537. astro-ph/0501152.

Bardeen JM, Bond JR, Kaiser N and Szalay AS (1986), May. The statistics of peaks of Gaussian random fields. *ApJ* 304: 15–61. doi:10.1086/164143.

Barreira A, Li B, Baugh CM and Pascoli S (2014), Aug. The observational status of Galileon gravity after Planck. *JCAP* 2014 (8): 059–059. doi:10.1088/1475-7516/2014/08/059. 1406.0485.

Barreira A, Cautun M, Li B, Baugh CM and Pascoli S (2015), Aug. Weak lensing by voids in modified lensing potentials. *JCAP* 8, 028. doi:10.1088/1475-7516/2015/08/028. 1505.05809.

Barreira A, Bose S, Li B and Llinares C (2017), Feb. Weak lensing by galaxy troughs with modified gravity. *JCAP* 2, 031. doi:10.1088/1475-7516/2017/02/031. 1605.08436.

Bayer AE, Villaescusa-Navarro F, Massara E, Liu J, Spergel DN, Verde L, Wandelt BD, Viel M and Ho S (2021), Sep. Detecting Neutrino Mass by Combining Matter Clustering, Halos, and Voids. *ApJ* 919 (1), 24. doi:10.3847/1538-4357/ac0e91. 2102.05049.

Bertschinger E (1985), May. The self-similar evolution of holes in an Einstein-de Sitter universe. *ApJS* 58: 1–37. doi:10.1086/191027.

Betancort-Rijo J, Patiri SG, Prada F and Romano AE (2009), Dec. The statistics of voids as a tool to constrain cosmological parameters: σ_8 and Γ. *MNRAS* 400 (4): 1835–1849. doi:10.1111/j.1365-2966.2009.15567.x. 0901.1609.

Blumenthal GR, da Costa LN, Goldwirth DS, Lecar M and Piran T (1992), Apr. The largest possible voids. *ApJ* 388: 234–241. doi:10.1086/171147.

Bond JR, Cole S, Efstathiou G and Kaiser N (1991), Oct. Excursion set mass functions for hierarchical Gaussian fluctuations. *ApJ* 379: 440–460. doi:10.1086/170520.

Bonici M, Carbone C, Davini S, Vielzeuf P, Paganin L, Cardone V, Hamaus N, Pisani A, Hawken AJ, Kovacs A, Nadathur S, Contarini S, Verza G, Tutusaus I, Marulli F, Moscardini L, Aubert M, Giocoli C, Pourtsidou A, Camera S, Escoffier S, Caminata A, Di Domizio S, Martinelli M, Pallavicini M, Pettorino V, Sakr Z, Sapone D, Testera G, Tosi S, Yankelevich V, Amara A, Auricchio N, Baldi M, Bonino D, Branchini E, Brescia M, Brinchmann J, Capobianco V, Carretero J, Castellano M, Cavuoti S, Cledassou R, Congedo G, Conversi L, Copin Y, Corcione L, Courbin F, Cropper M, Da Silva A, Degaudenzi H, Douspis M, Dubath F, Duncan CAJ, Dupac X, Dusini S, Ealet A, Farrens S, Ferriol S, Fosalba P, Frailis M, Franceschi E, Fumana M, Gómez-Alvarez P, Garilli B, Gillis B, Grazian A, Grupp F, Guzzo L, Haugan SVH, Holmes W, Hormuth F, Hornstrup A, Jahnke K, Kümmel M, Kermiche S, Kiessling A, Kilbinger M, Kunz M, Kurki-Suonio H, Laureijs R, Ligori S, Lilje PB, Lloro I, Maiorano E, Mansutti O, Marggraf O, Markovic K, Massey R, Medinaceli E, Melchior M, Meneghetti M, Meylan G, Moresco M, Munari E, Niemi SM, Padilla C, Paltani S, Pasian F, Pedersen K, Percival WJ, Pires S, Polenta G, Poncet M, Popa L, Raison F, Rebolo R, Renzi A, Rhodes J, Rossetti E, Saglia R, Sartoris B, Scodeggio M, Secroun A, Seidel G, Sirignano C, Sirri G, Stanco L, Starck JL, Surace C, Tallada-Crespí P, Tavagnacco D, Taylor AN, Tereno I, Toledo-Moreo R, Torradeflot F, Valentijn EA, Valenziano L, Wang Y, Weller J, Zamorani G, Zoubian J and Andreon S (2023), Feb. Euclid: Forecasts from the void-lensing cross-correlation. *A&A* 670, A47. doi:10.1051/0004-6361/202244445. 2206.14211.

Bos EGP, van de Weygaert R, Dolag K and Pettorino V (2012), Oct. The darkness that shaped the void: dark energy and cosmic voids. *MNRAS* 426: 440–461. doi:10.1111/j.1365-2966.2012.21478.x. 1205.4238.

Brouwer MM, Demchenko V, Harnois-Déraps J, Bilicki M, Heymans C, Hoekstra H, Kuijken K, Alpaslan M, Brough S, Cai YC, Costa-Duarte MV, Dvornik A, Erben T, Hildebrandt H, Holwerda BW, Schneider P, Sifón C and van Uitert E (2018), May. Studying galaxy troughs and ridges using Weak Gravitational Lensing with the Kilo-Degree Survey. *ArXiv e-prints* 1805.00562.

Burger PA, Friedrich O, Harnois-Déraps J, Schneider P, Asgari M, Bilicki M, Hildebrandt H, Wright AH, Castro T, Dolag K, Heymans C, Joachimi B, Kuijken K, Martinet N, Shan H and Tröster T (2023), Jan. KiDS-1000 cosmology: Constraints from density split statistics. *A&A* 669, A69. doi:10.1051/0004-6361/202244673. 2208.02171.

Cai YC, Neyrinck MC, Szapudi I, Cole S and Frenk CS (2014), May. A Possible Cold Imprint of Voids on the Microwave Background Radiation. *ApJ* 786, 110. doi:10.1088/0004-637X/786/2/110. 1301.6136.

Cai YC, Padilla N and Li B (2015), Jul. Testing gravity using cosmic voids. *MNRAS* 451: 1036–1055. doi:10.1093/mnras/stv777. 1410.1510.

Cai YC, Taylor A, Peacock JA and Padilla N (2016), Nov. Redshift-space distortions around voids. *MNRAS* 462: 2465–2477. doi:10.1093/mnras/stw1809. 1603.05184.

Cai YC, Neyrinck M, Mao Q, Peacock JA, Szapudi I and Berlind AA (2017), Apr. The lensing and temperature imprints of voids on the cosmic microwave background. *MNRAS* 466: 3364–3375. doi:10.1093/mnras/stw3299. 1609.00301.

Camacho-Ciurana G, Lee P, Arsenov N, Kovács A, Szapudi I and Csabai I (2023), Dec. The CMB lensing imprint of cosmic voids detected in the WISE-Pan-STARRS luminous red galaxy catalog. *arXiv e-prints* , arXiv:2312.08483doi:10.48550/arXiv.2312.08483. 2312.08483.

Cautun M, van de Weygaert R, Jones BJT and Frenk CS (2014), Jul. Evolution of the cosmic web. *MNRAS* 441 (4): 2923–2973. doi:10.1093/mnras/stu768. 1401.7866.

Cautun M, Paillas E, Cai YC, Bose S, Armijo J, Li B and Padilla N (2018), May. The Santiago-Harvard-Edinburgh-Durham void comparison - I. SHEDding light on chameleon gravity tests. *MNRAS* 476 (3): 3195–3217. doi:10.1093/mnras/sty463. 1710.01730.

Chantavat T, Sawangwit U and Wandelt BD (2017), Feb. Void Profile from Planck Lensing Potential Map. *ApJ* 836, 156. doi:10.3847/1538-4357/

836/2/156. 1702.01009.

Chuang CH, Kitaura FS, Liang Y, Font-Ribera A, Zhao C, McDonald P and Tao C (2017), Mar. Linear redshift space distortions for cosmic voids based on galaxies in redshift space. *Phys. Rev. D* 95 (6), 063528. doi:10.1103/PhysRevD.95.063528. 1605.05352.

Clampitt J and Jain B (2015), Dec. Lensing measurements of the mass distribution in SDSS voids. *MNRAS* 454: 3357–3365. doi:10.1093/mnras/stv2215. 1404.1834.

Clampitt J, Cai YC and Li B (2013). Voids in Modified Gravity: Excursion Set Predictions. *MNRAS* 431 (3): 749–766. doi:10.1093/mnras/stt219. 1212.2216.

Colberg JM, Sheth RK, Diaferio A, Gao L and Yoshida N (2005), Jun. Voids in a ΛCDM universe. *MNRAS* 360 (1): 216–226. doi:10.1111/j.1365-2966.2005.09064.x. astro-ph/0409162.

Colberg JM, Pearce F, Foster C, Platen E, Brunino R, Neyrinck M, Basilakos S, Fairall A, Feldman H, Gottlöber S, Hahn O, Hoyle F, Müller V, Nelson L, Plionis M, Porciani C, Shandarin S, Vogeley MS and van de Weygaert R (2008), Jun. The Aspen-Amsterdam void finder comparison project. *MNRAS* 387: 933–944. doi:10.1111/j.1365-2966.2008.13307.x. 0803.0918.

Contarini S, Ronconi T, Marulli F, Moscardini L, Veropalumbo A and Baldi M (2019), Sep. Cosmological exploitation of the size function of cosmic voids identified in the distribution of biased tracers. *MNRAS* 488 (3): 3526–3540. doi:10.1093/mnras/stz1989. 1904.01022.

Contarini S, Marulli F, Moscardini L, Veropalumbo A, Giocoli C and Baldi M (2021), Jul. Cosmic voids in modified gravity models with massive neutrinos. *MNRAS* 504 (4): 5021–5038. doi:10.1093/mnras/stab1112. 2009.03309.

Contarini S, Verza G, Pisani A, Hamaus N, Sahlén M, Carbone C, Dusini S, Marulli F, Moscardini L, Renzi A, Sirignano C, Stanco L, Aubert M, Bonici M, Castignani G, Courtois HM, Escoffier S, Guinet D, Kovacs A, Lavaux G, Massara E, Nadathur S, Pollina G, Ronconi T, Ruppin F, Sakr Z, Veropalumbo A, Wandelt BD, Amara A, Auricchio N, Baldi M, Bonino D, Branchini E, Brescia M, Brinchmann J, Camera S, Capobianco V, Carretero J, Castellano M, Cavuoti S, Cledassou R, Congedo G, Conselice CJ, Conversi L, Copin Y, Corcione L, Courbin F, Cropper M, Da Silva A, Degaudenzi H, Dubath F, Duncan CAJ, Dupac X, Ealet A, Farrens S, Ferriol S, Fosalba P, Frailis M, Franceschi E, Garilli B, Gillard W, Gillis B, Giocoli C, Grazian A, Grupp F, Guzzo L, Haugan S, Holmes W, Hormuth F, Jahnke K, Kümmel M, Kermiche S, Kiessling A, Kilbinger M, Kunz M, Kurki-Suonio H, Laureijs R, Ligori S, Lilje PB, Lloro I, Maiorano E, Mansutti O, Marggraf O, Markovic K, Massey R, Melchior M, Meneghetti M, Meylan G, Moresco M, Munari E, Niemi SM, Padilla C, Paltani S, Pasian F, Pedersen K, Percival WJ, Pettorino V, Pires S, Polenta G, Poncet M, Popa L, Pozzetti L, Raison F, Rhodes J, Rossetti E, Saglia R, Sartoris B, Schneider P, Secroun A, Seidel G, Sirri G, Surace C, Tallada-Crespí P, Taylor AN, Tereno I, Toledo-Moreo R, Torradeflot F, Valentijn EA, Valenziano L, Wang Y, Weller J, Zamorani G, Zoubian J, Andreon S, Maino D and Mei S (2022), Nov. Euclid: Cosmological forecasts from the void size function. *A&A* 667, A162. doi:10.1051/0004-6361/202244095. 2205.11525.

Contarini S, Pisani A, Hamaus N, Marulli F, Moscardini L and Baldi M (2023), Aug. Cosmological Constraints from the BOSS DR12 Void Size Function. *ApJ* 953 (1), 46. doi:10.3847/1538-4357/acde54. 2212.03873.

Contarini S, Pisani A, Hamaus N, Marulli F, Moscardini L and Baldi M (2024), Feb. The perspective of voids on rising cosmology tensions. *A&A* 682, A20. doi:10.1051/0004-6361/202347572. 2212.07438.

Correa CM, Paz DJ, Padilla ND, Sánchez AG, Ruiz AN and Angulo RE (2022), Jan. Redshift-space effects in voids and their impact on cosmological tests - II. The void-galaxy cross-correlation function. *MNRAS* 509 (2): 1871–1884. doi:10.1093/mnras/stab3070. 2107.01314.

Coulton WR, Liu J, McCarthy IG and Osato K (2020), Jul. Weak lensing minima and peaks: Cosmological constraints and the impact of baryons. *MNRAS* 495 (3): 2531–2542. doi:10.1093/mnras/staa1098. 1910.04171.

Cruz M, Martínez-González E, Vielva P and Cayón L (2005), Jan. Detection of a non-Gaussian spot in WMAP. *MNRAS* 356: 29–40. doi:10.1111/j.1365-2966.2004.08419.x. astro-ph/0405341.

Davies CT, Cautun M and Li B (2019), Dec. Cosmological test of gravity using weak lensing voids. *MNRAS* 490 (4): 4907–4917. doi:10.1093/mnras/stz2933. 1907.06657.

Davies CT, Cautun M, Giblin B, Li B, Harnois-Déraps J and Cai YC (2021), Oct. Constraining cosmology with weak lensing voids. *MNRAS* 507 (2): 2267–2282. doi:10.1093/mnras/stab2251. 2010.11954.

Demchenko V, Cai YC, Heymans C and Peacock JA (2016), Nov. Testing the spherical evolution of cosmic voids. *MNRAS* 463: 512–519. doi:10.1093/mnras/stw2030. 1605.05286.

Demirbozan U, Nadathur S, Ferrero I, Fosalba P, Kovacs A, Miquel R, Davies CT, Pandey S, Adamow M, Bechtol K, Drlica-Wagner A, Gruendl R, Hartley W, Pieres A, Ross A, Rykoff E, Sheldon E, Yanny B, Abbott T, Aguena M, Allam S, Alves O, Bacon D, Bertin E, Bocquet S, Brooks D, Carnero Rosell A, Carretero J, Cawthon R, da Costa L, Elidaiana da Silva Pereira M, De Vicente J, Desai S, Doel P, Everett S, Flaugher B, Friedel D, Frieman J, Gatti M, Gaztanaga E, Giannini G, Gutierrez G, Hinton S, Hollowood DL, James D, Jeffrey N, Kuehn K, Lahav O, Lee S, Marshall J, Mena-Fernández J, Mohr J, Myles J, Ogando R, Plazas Malagón A, Roodman A, Sanchez E, Sevilla I, Smith M, Soares-Santos M, Suchyta E, Swanson M, Tarle G, Weaverdyck N, Weller J and Wiseman P (2024), Apr. The Gravitational Lensing Imprints of DES Y3 Superstructures on the CMB: A Matched Filtering Approach. *arXiv e-prints* , arXiv:2404.18278doi:10.48550/arXiv.2404.18278. 2404.18278.

DESI Collaboration, Aghamousa A, Aguilar J, Ahlen S, Alam S, Allen LE, Allende Prieto C, Annis J, Bailey S, Balland C, Ballester O, Baltay C, Beaufore L, Bebek C, Beers TC, Bell EF, Bernal JL, Besuner R, Beutler F, Blake C, Bleuler H, Blomqvist M, Blum R, Bolton AS, Briceno C, Brooks D, Brownstein JR, Buckley-Geer E, Burden A, Burtin E, Busca NG, Cahn RN, Cai YC, Cardiel-Sas L, Carlberg RG, Carton PH, Casas R, Castander FJ, Cervantes-Cota JL, Claybaugh TM, Close M, Coker CT, Cole S, Comparat J, Cooper AP, Cousinou MC, Crocce M, Cuby JG, Cunningham DP, Davis TM, Dawson KS, de la Macorra A, De Vicente J, Delubac T, Derwent M, Dey A, Dhungana G, Ding Z, Doel P, Duan YT, Ealet A, Edelstein J, Eftekharzadeh S, Eisenstein DJ, Elliott A, Escoffier S, Evatt M, Fagrelius P, Fan X, Fanning K, Farahi A, Farihi J, Favole G, Feng Y, Fernandez E, Findlay JR, Finkbeiner DP, Fitzpatrick MJ, Flaugher B, Flender S, Font-Ribera A, Forero-Romero JE, Fosalba P, Frenk CS, Fumagalli M, Gaensicke BT, Gallo G, Garcia-Bellido J, Gaztanaga E, Pietro Gentile Fusillo N, Gerard T, Gershkovich I, Giannantonio T, Gillet D, Gonzalez-de-Rivera G, Gonzalez-Perez V, Gott S, Graur O, Gutierrez G, Guy J, Habib S, Heetderks H, Heetderks I, Heitmann K, Hellwing WA, Herrera DA, Ho S, Holland S, Honscheid K, Huff E, Hutchinson TA, Huterer D, Hwang HS, Illa Laguna JM, Ishikawa Y, Jacobs D, Jeffrey N, Jelinsky P, Jennings E, Jiang L, Jimenez J, Johnson J, Joyce R, Jullo E, Juneau S, Kama S, Karcher A, Karkar S, Kehoe R, Kennamer N, Kent S, Kilbinger M, Kim AG, Kirkby D, Kisner T, Kitanidis E, Kneib JP, Koposov S, Kovacs E, Koyama K, Kremin A, Kron R, Kronig L, Kueter-Young A, Lacey CG, Lafever R, Lahav O, Lambert A, Lampton M, Landriau M, Lang D, Lauer TR, Le Goff JM, Le Guillou L, Le Van Suu A, Lee JH, Lee SJ, Leitner D, Lesser M, Levi ME, L'Huillier B, Li B, Liang M, Lin H, Linder E, Loebman SR, Lukić Z, Ma J, MacCrann N, Magneville C, Makarem L, Manera M, Manser CJ, Marshall R, Martini P, Massey R, Matheson T, McCauley J, McDonald P, McGreer ID, Meisner A, Metcalfe N, Miller TN, Miquel R, Moustakas J, Myers A, Naik M, Newman JA, Nichol RC, Nicola A, Nicolati da Costa L, Nie J, Niz G, Norberg P, Nord B, Norman D, Nugent P, O'Brien T, Oh M, Olsen KAG, Padilla C, Padmanabhan H, Padmanabhan N, Palanque-Delabrouille N, Palmese A, Pappalardo D, Pâris I, Park C, Patej A, Peacock JA, Peiris HV, Peng X, Percival WJ, Perruchot S, Pieri M, Pogge R, Pollack JE, Poppett C, Prada F, Prakash A, Probst RG, Rabinowitz D, Raichoor A, Ree CH, Refregier A, Regal X, Reid B, Reil K, Rezaie M, Rockosi CM, Roe N, Ronayette S, Roodman A, Ross AJ, Ross NP, Rossi G, Rozo E, Ruhlmann-Kleider V, Rykoff ES, Sabiu C, Samushia L, Sanchez E, Sanchez J, Schlegel DJ, Schneider M, Schubnell M, Secroun A, Seljak U, Seo HJ, Serrano S, Shafieloo A, Shan H, Sharples R, Sholl MJ, Shourt WV, Silber JH, Silva DR, Sirk MM, Slosar A, Smith A, Smoot GF, Som D, Song YS, Sprayberry

D, Staten R, Stefanik A, Tarle G, Sien Tie S, Tinker JL, Tojeiro R, Valdes F, Valenzuela O, Valluri M, Vargas-Magana M, Verde L, Walker AR, Wang J, Wang Y, Weaver BA, Weaverdyck C, Wechsler RH, Weinberg DH, White M, Yang Q, Yeche C, Zhang T, Zhao GB, Zheng Y, Zhou X, Zhou Z, Zhu Y, Zou H and Zu Y (2016), Oct. The DESI Experiment Part I: Science,Targeting, and Survey Design. *arXiv e-prints* , arXiv:1611.00036doi:10.48550/arXiv.1611.00036. 1611.00036.

Dong F, Yu Y, Zhang J, Yang X and Zhang P (2021a), Jan. Measuring the integrated Sachs-Wolfe effect from the low-density regions of the universe. *MNRAS* 500 (3): 3838–3853. doi:10.1093/mnras/staa3194. 2006.14202.

Dong F, Zhang P, Zhang L, Yao J, Sun Z, Park C and Yang X (2021b), Dec. Detection of a Cross-correlation between Cosmic Microwave Background Lensing and Low-density Points. *ApJ* 923 (2), 153. doi:10.3847/1538-4357/ac2d31. 2107.08694.

Douglass KA, Veyrat D and BenZvi S (2023), Mar. Updated Void Catalogs of the SDSS DR7 Main Sample. *ApJS* 265 (1), 7. doi:10.3847/1538-4365/acabcf. 2202.01226.

Falck BL, Neyrinck MC and Szalay AS (2012), Aug. ORIGAMI: Delineating Halos Using Phase-space Folds. *ApJ* 754 (2), 126. doi:10.1088/0004-637X/754/2/126. 1201.2353.

Falck B, Koyama K, Zhao Gb and Li B (2014), Jul. The Vainshtein mechanism in the cosmic web. *JCAP* 7, 058. doi:10.1088/1475-7516/2014/07/058. 1404.2206.

Falck B, Koyama K and Zhao GB (2015), Jul. Cosmic web and environmental dependence of screening: Vainshtein vs. chameleon. *JCAP* 7, 049. doi:10.1088/1475-7516/2015/07/049. 1503.06673.

Fang Y, Hamaus N, Jain B, Pandey S, Pollina G, Sánchez C, Kovács A, Chang C, Carretero J, Castander FJ, Choi A, Crocce M, DeRose J, Fosalba P, Gatti M, Gaztañaga E, Gruen D, Hartley WG, Hoyle B, MacCrann N, Prat J, Rau MM, Rykoff ES, Samuroff S, Sheldon E, Troxel MA, Vielzeuf P, Zuntz J, Annis J, Avila S, Bertin E, Brooks D, Burke DL, Carnero Rosell A, Carrasco Kind M, Cawthon R, da Costa LN, De Vicente J, Desai S, Diehl HT, Dietrich JP, Doel P, Everett S, Evrard AE, Flaugher B, Frieman J, García-Bellido J, Gerdes DW, Gruendl RA, Gutierrez G, Hollowood DL, James DJ, Jarvis M, Kuropatkin N, Lahav O, Maia MAG, Marshall JL, Melchior P, Menanteau F, Miquel R, Palmese A, Plazas AA, Romer AK, Roodman A, Sanchez E, Serrano S, Sevilla-Noarbe I, Smith M, Soares-Santos M, Sobreira F, Suchyta E, Swanson MEC, Tarle G, Thomas D, Vikram V, Walker AR, Weller J and DES Collaboration (2019), Dec. Dark Energy Survey year 1 results: the relationship between mass and light around cosmic voids. *MNRAS* 490 (3): 3573–3587. doi:10.1093/mnras/stz2805. 1909.01386.

Fernández-García E, Betancort-Rijo JE, Prada F, Ishiyama T and Klypin A (2024), Jun. Constraining cosmological parameters using void statistics from the SDSS survey. *arXiv e-prints* , arXiv:2406.13736doi:10.48550/arXiv.2406.13736. 2406.13736.

Fisher KB (1995), Aug. On the Validity of the Streaming Model for the Redshift-Space Correlation Function in the Linear Regime. *ApJ* 448: 494. doi:10.1086/175980. astro-ph/9412081.

Flender S, Hotchkiss S and Nadathur S (2013), Feb. The stacked ISW signal of rare superstructures in ΛCDM. *JCAP* 2, 013. doi:10.1088/1475-7516/2013/02/013. 1212.0776.

Forero-Romero JE, Hoffman Y, Gottlöber S, Klypin A and Yepes G (2009), Jul. A dynamical classification of the cosmic web. *MNRAS* 396 (3): 1815–1824. doi:10.1111/j.1365-2966.2009.14885.x. 0809.4135.

Fraser TS, Paillas E, Percival WJ, Nadathur S, Radinović S and Winther HA (2024), Jul. Modelling the BOSS void-galaxy cross-correlation function using a neural-network emulator. *arXiv e-prints* , arXiv:2407.03221doi:10.48550/arXiv.2407.03221. 2407.03221.

Friedrich O, Gruen D, DeRose J, Kirk D, Krause E, McClintock T, Rykoff ES, Seitz S, Wechsler RH, Bernstein GM, Blazek J, Chang C, Hilbert S, Jain B, Kovacs A, Lahav O, Abdalla FB, Allam S, Annis J, Bechtol K, Benoit-Lévy A, Bertin E, Brooks D, Carnero Rosell A, Carrasco Kind M, Carretero J, Cunha CE, D'Andrea CB, da Costa LN, Davis C, Desai S, Diehl HT, Dietrich JP, Drlica-Wagner A, Eifler TF, Fosalba P, Frieman J, García-Bellido J, Gaztanaga E, Gerdes DW, Giannantonio T, Gruendl RA, Gschwend J, Gutierrez G, Honscheid K, James DJ, Jarvis M, Kuehn K, Kuropatkin N, Lima M, March M, Marshall JL, Melchior P, Menanteau F, Miquel R, Mohr JJ, Nord B, Plazas AA, Sanchez E, Scarpine V, Schindler R, Schubnell M, Sevilla-Noarbe I, Sheldon E, Smith M, Soares-Santos M, Sobreira F, Suchyta E, Swanson MEC, Tarle G, Thomas D, Troxel MA, Vikram V, Weller J and DES Collaboration (2018), Jul. Density split statistics: Joint model of counts and lensing in cells. *Phys. Rev. D* 98 (2), 023508. doi:10.1103/PhysRevD.98.023508. 1710.05162.

Garcia-Bellido J and Haugbølle T (2008), Apr. Confronting Lemaitre Tolman Bondi models with observational cosmology. *JCAP* 2008 (4), 003. doi:10.1088/1475-7516/2008/04/003. 0802.1523.

Granett BR, Neyrinck MC and Szapudi I (2008), Aug. An Imprint of Superstructures on the Microwave Background due to the Integrated Sachs-Wolfe Effect. *ApJ* 683: L99. doi:10.1086/591670. 0805.3695.

Gregory SA and Thompson LA (1978), Jun. The Coma/A1367 supercluster and its environs. *ApJ* 222: 784–799. doi:10.1086/156198.

Gruen D, Friedrich O, Amara A, Bacon D, Bonnett C, Hartley W, Jain B, Jarvis M, Kacprzak T, Krause E, Mana A, Rozo E, Rykoff ES, Seitz S, Sheldon E, Troxel MA, Vikram V, Abbott TMC, Abdalla FB, Allam S, Armstrong R, Banerji M, Bauer AH, Becker MR, Benoit-Lévy A, Bernstein GM, Bernstein RA, Bertin E, Bridle SL, Brooks D, Buckley-Geer E, Burke DL, Capozzi D, Carnero Rosell A, Carrasco Kind M, Carretero J, Crocce M, Cunha CE, D'Andrea CB, da Costa LN, DePoy DL, Desai S, Diehl HT, Dietrich JP, Doel P, Eifler TF, Neto AF, Fernandez E, Flaugher B, Fosalba P, Frieman J, Gerdes DW, Gruendl RA, Gutierrez G, Honscheid K, James DJ, Kuehn K, Kuropatkin N, Lahav O, Li TS, Lima M, Maia MAG, March M, Martini P, Melchior P, Miller CJ, Miquel R, Mohr JJ, Nord B, Ogando R, Plazas AA, Reil K, Romer AK, Roodman A, Sako M, Sanchez E, Scarpine V, Schubnell M, Sevilla-Noarbe I, Smith RC, Soares-Santos M, Sobreira F, Suchyta E, Swanson MEC, Tarle G, Thaler J, Thomas D, Walker AR, Wechsler RH, Weller J, Zhang Y and Zuntz J (2016), Jan. Weak lensing by galaxy troughs in DES Science Verification data. *MNRAS* 455: 3367–3380. doi:10.1093/mnras/stv2506. 1507.05090.

Gruen D, Friedrich O, Krause E, DeRose J, Cawthon R, Davis C, Elvin-Poole J, Rykoff ES, Wechsler RH, Alarcon A, Bernstein GM, Blazek J, Chang C, Clampitt J, Crocce M, De Vicente J, Gatti M, Gill MSS, Hartley WG, Hilbert S, Hoyle B, Jain B, Jarvis M, Lahav O, MacCrann N, McClintock T, Prat J, Rollins RP, Ross AJ, Rozo E, Samuroff S, Sánchez C, Sheldon E, Troxel MA, Zuntz J, Abbott TMC, Abdalla FB, Allam S, Annis J, Bechtol K, Benoit-Lévy A, Bertin E, Bridle SL, Brooks D, Buckley-Geer E, Carnero Rosell A, Carrasco Kind M, Carretero J, Cunha CE, D'Andrea CB, da Costa LN, Desai S, Diehl HT, Dietrich JP, Doel P, Drlica-Wagner A, Fernandez E, Flaugher B, Fosalba P, Frieman J, García-Bellido J, Gaztanaga E, Giannantonio T, Gruendl RA, Gschwend J, Gutierrez G, Honscheid K, James DJ, Jeltema T, Kuehn K, Kuropatkin N, Lima M, March M, Marshall JL, Martini P, Melchior P, Menanteau F, Miquel R, Mohr JJ, Plazas AA, Roodman A, Sanchez E, Scarpine V, Schubnell M, Sevilla-Noarbe I, Smith M, Smith RC, Soares-Santos M, Sobreira F, Swanson MEC, Tarle G, Thomas D, Vikram V, Walker AR, Weller J, Zhang Y and DES Collaboration (2018), Jul. Density split statistics: Cosmological constraints from counts and lensing in cells in DES Y1 and SDSS data. *Phys. Rev. D* 98 (2), 023507. doi:10.1103/PhysRevD.98.023507. 1710.05045.

Guth AH (1981), Jan. Inflationary universe: A possible solution to the horizon and flatness problems. *Phys. Rev. D* 23 (2): 347–356. doi:10.1103/PhysRevD.23.347.

Hahn O, Porciani C, Carollo CM and Dekel A (2007), Feb. Properties of dark matter haloes in clusters, filaments, sheets and voids. *MNRAS* 375 (2): 489–499. doi:10.1111/j.1365-2966.2006.11318.x. astro-ph/0610280.

Hamaus N, Sutter PM, Lavaux G and Wandelt BD (2014a), Dec. Testing cosmic geometry without dynamic distortions using voids. *JCAP* 2014 (12): 013–013. doi:10.1088/1475-7516/2014/12/013. 1409.3580.

Hamaus N, Sutter PM and Wandelt BD (2014b), Jun. Universal Density Profile for Cosmic Voids. *Phys. Rev. Lett.* 112 (25), 251302. doi:

10.1103/PhysRevLett.112.251302. 1403.5499.

Hamaus N, Sutter PM, Lavaux G and Wandelt BD (2015), Nov. Probing cosmology and gravity with redshift-space distortions around voids. *JCAP* 11, 036. doi:10.1088/1475-7516/2015/11/036. 1507.04363.

Hamaus N, Pisani A, Sutter PM, Lavaux G, Escoffier S, Wandelt BD and Weller J (2016), Aug. Constraints on Cosmology and Gravity from the Dynamics of Voids. *Physical Review Letters* 117 (9), 091302. doi:10.1103/PhysRevLett.117.091302. 1602.01784.

Hamaus N, Cousinou MC, Pisani A, Aubert M, Escoffier S and Weller J (2017), Jul. Multipole analysis of redshift-space distortions around cosmic voids. *JCAP* 7, 014. doi:10.1088/1475-7516/2017/07/014. 1705.05328.

Hamaus N, Pisani A, Choi JA, Lavaux G, Wandelt BD and Weller J (2020), Dec. Precision cosmology with voids in the final BOSS data. *JCAP* 2020 (12), 023. doi:10.1088/1475-7516/2020/12/023. 2007.07895.

Hamaus N, Aubert M, Pisani A, Contarini S, Verza G, Cousinou MC, Escoffier S, Hawken A, Lavaux G, Pollina G, Wandelt BD, Weller J, Bonici M, Carbone C, Guzzo L, Kovacs A, Marulli F, Massara E, Moscardini L, Ntelis P, Percival WJ, Radinović S, Sahlén M, Sakr Z, Sánchez AG, Winther HA, Auricchio N, Awan S, Bender R, Bodendorf C, Bonino D, Branchini E, Brescia M, Brinchmann J, Capobianco V, Carretero J, Castander FJ, Castellano M, Cavuoti S, Cimatti A, Cledassou R, Congedo G, Conversi L, Copin Y, Corcione L, Cropper M, Da Silva A, Degaudenzi H, Douspis M, Dubath F, Duncan CAJ, Dupac X, Dusini S, Ealet A, Ferriol S, Fosalba P, Frailis M, Franceschi E, Franzetti P, Fumana M, Garilli B, Gillis B, Giocoli C, Grazian A, Grupp F, Haugan SVH, Holmes W, Hormuth F, Jahnke K, Kermiche S, Kiessling A, Kilbinger M, Kitching T, Kümmel M, Kunz M, Kurki-Suonio H, Ligori S, Lilje PB, Lloro I, Maiorano E, Marggraf O, Markovic K, Massey R, Maurogordato S, Melchior M, Meneghetti M, Meylan G, Moresco M, Munari E, Niemi SM, Padilla C, Paltani S, Pasian F, Pedersen K, Pettorino V, Pires S, Poncet M, Popa L, Pozzetti L, Rebolo R, Rhodes J, Rix H, Roncarelli M, Rossetti E, Saglia R, Schneider P, Secroun A, Seidel G, Serrano S, Sirignano C, Sirri G, Starck JL, Tallada-Crespí P, Tavagnacco D, Taylor AN, Tereno I, Toledo-Moreo R, Torradeflot F, Valentijn EA, Valenziano L, Wang Y, Welikala N, Zamorani G, Zoubian J, Andreon S, Baldi M, Camera S, Mei S, Neissner C and Romelli E (2022), Feb. Euclid: Forecasts from redshift-space distortions and the Alcock-Paczynski test with cosmic voids. *A&A* 658, A20. doi:10.1051/0004-6361/202142073. 2108.10347.

Hang Q, Alam S, Cai YC and Peacock JA (2021), Oct. Stacked CMB lensing and ISW signals around superstructures in the DESI Legacy Survey. *MNRAS* 507 (1): 510–523. doi:10.1093/mnras/stab2184. 2105.11936.

Hawken AJ, Granett BR, Iovino A, Guzzo L, Peacock JA, de la Torre S, Garilli B, Bolzonella M, Scodeggio M, Abbas U, Adami C, Bottini D, Cappi A, Cucciati O, Davidzon I, Fritz A, Franzetti P, Krywult J, Le Brun V, Le Fèvre O, Maccagni D, Małek K, Marulli F, Polletta M, Pollo A, Tasca LAM, Tojeiro R, Vergani D, Zanichelli A, Arnouts S, Bel J, Branchini E, De Lucia G, Ilbert O, Moscardini L and Percival WJ (2017), Nov. The VIMOS Public Extragalactic Redshift Survey. Measuring the growth rate of structure around cosmic voids. *A&A* 607, A54. doi:10.1051/0004-6361/201629678. 1611.07046.

Hawken AJ, Aubert M, Pisani A, Cousinou MC, Escoffier S, Nadathur S, Rossi G and Schneider DP (2020), Jun. Constraints on the growth of structure around cosmic voids in eBOSS DR14. *JCAP* 2020 (6), 012. doi:10.1088/1475-7516/2020/06/012. 1909.04394.

Hidding J, van de Weygaert R and Shandarin S (2016), Oct., The Zeldovich & Adhesion approximations and applications to the local universe, van de Weygaert R, Shandarin S, Saar E and Einasto J, (Eds.), The Zeldovich Universe: Genesis and Growth of the Cosmic Web, IAU Symposium, 308, 69–76, 1611.01221.

Higuchi Y, Oguri M and Hamana T (2013), Jun. Measuring the mass distribution of voids with stacked weak lensing. *MNRAS* 432: 1021–1031. doi:10.1093/mnras/stt521. 1211.5966.

Hoffman Y, Metuki O, Yepes G, Gottlöber S, Forero-Romero JE, Libeskind NI and Knebe A (2012), Sep. A kinematic classification of the cosmic web. *MNRAS* 425: 2049–2057. doi:10.1111/j.1365-2966.2012.21553.x. 1201.3367.

Hoyle F and Vogeley MS (2002), Feb. Voids in the Point Source Catalogue Survey and the Updated Zwicky Catalog. *ApJ* 566 (2): 641–651. doi:10.1086/338340. astro-ph/0109357.

Hoyle F and Vogeley MS (2004), Jun. Voids in the Two-Degree Field Galaxy Redshift Survey. *ApJ* 607 (2): 751–764. doi:10.1086/386279. astro-ph/0312533.

Hu W and Sawicki I (2007), Sep. Models of f(R) cosmic acceleration that evade solar system tests. *Phys. Rev. D* 76 (6), 064004. doi:10.1103/PhysRevD.76.064004. 0705.1158.

Icke V (1984), Jan. Voids and filaments. *MNRAS* 206: 1P–3P. doi:10.1093/mnras/206.1.1P.

Icke V and van de Weygaert R (1991), Jun. The galaxy distribution as a Voronoi foam. *QJRAS* 32: 85–112.

Ilić S, Langer M and Douspis M (2013), Aug. Detecting the integrated Sachs-Wolfe effect with stacked voids. *A&A* 556, A51. doi:10.1051/0004-6361/201321150. 1301.5849.

Jõeveer M, Einasto J and Tago E (1978), Nov. Spatial distribution of galaxies and of clusters of galaxies in the southern galactic hemisphere. *MNRAS* 185: 357–370. doi:10.1093/mnras/185.2.357.

Jaber M, Peper M, Hellwing WA, Aragón-Calvo MA and Valenzuela O (2024), Jan. Hierarchical structure of the cosmic web and galaxy properties. *MNRAS* 527 (2): 4087–4099. doi:10.1093/mnras/stad3347. 2304.14387.

Jennings E, Li Y and Hu W (2013), Sep. The abundance of voids and the excursion set formalism. *MNRAS* 434: 2167–2181. doi:10.1093/mnras/stt1169. 1304.6087.

Kaiser N (1987), Jul. Clustering in real space and in redshift space. *MNRAS* 227: 1–21. doi:10.1093/mnras/227.1.1.

Kaiser N (2017), Jul. Why there is no Newtonian backreaction. *MNRAS* 469 (1): 744–748. doi:10.1093/mnras/stx907. 1703.08809.

Keenan RC, Barger AJ and Cowie LL (2013), Sep. Evidence for a ~300 Megaparsec Scale Under-density in the Local Galaxy Distribution. *ApJ* 775 (1), 62. doi:10.1088/0004-637X/775/1/62. 1304.2884.

Kenworthy WD, Scolnic D and Riess A (2019), Apr. The Local Perspective on the Hubble Tension: Local Structure Does Not Impact Measurement of the Hubble Constant. *ApJ* 875 (2), 145. doi:10.3847/1538-4357/ab0ebf. 1901.08681.

Kitaura FS, Chuang CH, Liang Y, Zhao C, Tao C, Rodríguez-Torres S, Eisenstein DJ, Gil-Marín H, Kneib JP, McBride C, Percival WJ, Ross AJ, Sánchez AG, Tinker J, Tojeiro R, Vargas-Magana M and Zhao GB (2016), Apr. Signatures of the Primordial Universe from Its Emptiness: Measurement of Baryon Acoustic Oscillations from Minima of the Density Field. *Physical Review Letters* 116 (17), 171301. doi:10.1103/PhysRevLett.116.171301. 1511.04405.

Kovács A (2018), Apr. The part and the whole: voids, supervoids, and their ISW imprint. *MNRAS* 475: 1777–1790. doi:10.1093/mnras/stx3213. 1701.08583.

Kovács A and Granett BR (2015), Sep. Cold imprint of supervoids in the cosmic microwave background re-considered with Planck and Baryon Oscillation Spectroscopic Survey DR10. *MNRAS* 452: 1295–1302. doi:10.1093/mnras/stv1371. 1501.03376.

Kovács A, Sánchez C, García-Bellido J, Elvin-Poole J, Hamaus N, Miranda V, Nadathur S, Abbott T, Abdalla FB, Annis J, Avila S, Bertin E, Brooks D, Burke DL, Carnero Rosell A, Carrasco Kind M, Carretero J, Cawthon R, Crocce M, Cunha C, da Costa LN, Davis C, De Vicente J, DePoy D, Desai S, Diehl HT, Doel P, Fernandez E, Flaugher B, Fosalba P, Frieman J, Gaztañaga E, Gerdes D, Gruendl R, Gutierrez G, Hartley W, Hollowood DL, Honscheid K, Hoyle B, James DJ, Krause E, Kuehn K, Kuropatkin N, Lahav O, Lima M, Maia M, March M, Marshall J, Melchior P, Menanteau F, Miller CJ, Miquel R, Mohr J, Plazas AA, Romer K, Rykoff E, Sanchez E, Scarpine V, Schindler R, Schubnell

M, Sevilla-Noarbe I, Smith M, Smith RC, Soares-Santos M, Sobreira F, Suchyta E, Swanson M, Tarle G, Thomas D, Vikram V, Weller J and DES Collaboration (2019), Apr. More out of less: an excess integrated Sachs-Wolfe signal from supervoids mapped out by the Dark Energy Survey. *MNRAS* 484 (4): 5267–5277. doi:10.1093/mnras/stz341. 1811.07812.

Kovács A, Beck R, Smith A, Rácz G, Csabai I and Szapudi I (2022a), Jun. Evidence for a high-z ISW signal from supervoids in the distribution of eBOSS quasars. *MNRAS* 513 (1): 15–26. doi:10.1093/mnras/stac903. 2107.13038.

Kovács A, Jeffrey N, Gatti M, Chang C, Whiteway L, Hamaus N, Lahav O, Pollina G, Bacon D, Kacprzak T, Mawdsley B, Nadathur S, Zeurcher D, García-Bellido J, Alarcon A, Amon A, Bechtol K, Bernstein GM, Campos A, Carnero Rosell A, Carrasco Kind M, Cawthon R, Chen R, Choi A, Cordero J, Davis C, DeRose J, Doux C, Drlica-Wagner A, Eckert K, Elsner F, Elvin-Poole J, Everett S, Ferté A, Giannini G, Gruen D, Gruendl RA, Harrison I, Hartley WG, Herner K, Huff EM, Huterer D, Kuropatkin N, Jarvis M, Leget PF, MacCrann N, McCullough J, Muir J, Myles J, Navarro-Alsina A, Pandey S, Prat J, Raveri M, Rollins RP, Ross AJ, Rykoff ES, Sánchez C, Secco LF, Sevilla-Noarbe I, Sheldon E, Shin T, Troxel MA, Tutusaus I, Varga TN, Yanny B, Yin B, Zhang Y, Zuntz J, Aguena M, Allam S, Andrade-Oliveira F, Annis J, Bertin E, Brooks D, Burke D, Carretero J, Costanzi M, da Costa LN, Pereira MES, Davis T, De Vicente J, Desai S, Diehl HT, Ferrero I, Flaugher B, Fosalba P, Frieman J, Gaztañaga E, Gerdes D, Giannantonio T, Gschwend J, Gutierrez G, Hinton S, Hollowood DL, Honscheid K, James D, Kuehn K, Lima M, Maia MAG, Marshall JL, Melchior P, Menanteau F, Miquel R, Morgan R, Ogando R, Paz-Chinchon F, Pieres A, Plazas AA, Monroy MR, Romer K, Roodman A, Sanchez E, Schubnell M, Serrano S, Smith M, Soares-Santos M, Suchyta E, Swanson MEC, Tarle G, Thomas D, To CH and Weller J (2022b), Feb. The DES view of the Eridanus supervoid and the CMB cold spot. *MNRAS* 510 (1): 216–229. doi:10.1093/mnras/stab3309. 2112.07699.

Kovács A, Vielzeuf P, Ferrero I, Fosalba P, Demirbozan U, Miquel R, Chang C, Hamaus N, Pollina G, Bechtol K, Becker M, Carnero Rosell A, Carrasco Kind M, Cawthon R, Crocce M, Drlica-Wagner A, Elvin-Poole J, Gatti M, Giannini G, Gruendl RA, Porredon A, Ross AJ, Rykoff ES, Sevilla-Noarbe I, Sheldon E, Yanny B, Abbott T, Aguena M, Allam S, Annis J, Bacon D, Bernstein G, Bertin E, Bocquet S, Brooks D, Burke D, Carretero J, Castander FJ, Costanzi M, da Costa LN, Pereira MES, De Vicente J, Desai S, Diehl HT, Dietrich J, Ferté A, Flaugher B, Frieman J, Garcia-Bellido J, Gaztañaga E, Gerdes D, Giannantonio T, Gruen D, Gschwend J, Gutierrez G, Hinton S, Hollowood DL, Honscheid K, Huterer D, Kuehn K, Lahav O, Lima M, March M, Marshall J, Melchior P, Menanteau F, Morgan R, Muir J, Ogando R, Palmese A, Paz-Chinchon F, Pieres A, Plazas Malagón A, Rodriguez Monroy M, Roodman A, Sanchez E, Schubnell M, Serrano S, Smith M, Suchyta E, Tarle G, Thomas D, To CH, Varga TN, Weller J and DES Collaboration (2022c), Sep. Dark Energy Survey Year 3 results: Imprints of cosmic voids and superclusters in the Planck CMB lensing map. *MNRAS* 515 (3): 4417–4429. doi:10.1093/mnras/stac2011. 2203.11306.

Krause E, Chang TC, Doré O and Umetsu K (2013), Jan. The Weight of Emptiness: The Gravitational Lensing Signal of Stacked Voids. *ApJ* 762, L20. doi:10.1088/2041-8205/762/2/L20. 1210.2446.

Kreisch CD, Pisani A, Carbone C, Liu J, Hawken AJ, Massara E, Spergel DN and Wandelt BD (2019), Sep. Massive neutrinos leave fingerprints on cosmic voids. *MNRAS* 488 (3): 4413–4426. doi:10.1093/mnras/stz1944. 1808.07464.

Krolewski A, Lee KG, White M, Hennawi JF, Schlegel DJ, Nugent PE, Lukić Z, Stark CW, Koekemoer AM, Le Fèvre O, Lemaux BC, Maier C, Rich RM, Salvato M and Tasca L (2018), Jul. Detection of z ∼ 2.3 Cosmic Voids from 3D Lyα Forest Tomography in the COSMOS Field. *ApJ* 861 (1), 60. doi:10.3847/1538-4357/aac829. 1710.02612.

Lam TY, Clampitt J, Cai YC and Li B (2015), Jul. Voids in modified gravity reloaded: Eulerian void assignment. *MNRAS* 450: 3319–3330. doi:10.1093/mnras/stv797. 1408.5338.

Lavaux G and Wandelt BD (2010), Apr. Precision cosmology with voids: definition, methods, dynamics. *MNRAS* 403: 1392–1408. doi:10.1111/j.1365-2966.2010.16197.x. 0906.4101.

Lavaux G and Wandelt BD (2012), Aug. Precision Cosmography with Stacked Voids. *APJ* 754, 109. doi:10.1088/0004-637X/754/2/109. 1110.0345.

Lee J and Park D (2009), May. Constraining the Dark Energy Equation of State with Cosmic Voids. *APJL* 696: L10–L12. doi:10.1088/0004-637X/696/1/L10. 0704.0881.

Li G, Ma YZ, Tramonte D and Li GL (2024), Jan. Cross-correlation of cosmic voids with thermal Sunyaev-Zel'dovich data. *MNRAS* 527 (2): 2663–2671. doi:10.1093/mnras/stad3396. 2311.00826.

Liang Y, Zhao C, Chuang CH, Kitaura FS and Tao C (2016), Jul. Measuring baryon acoustic oscillations from the clustering of voids. *MNRAS* 459: 4020–4028. doi:10.1093/mnras/stw884. 1511.04391.

Libeskind NI, van de Weygaert R, Cautun M, Falck B, Tempel E, Abel T, Alpaslan M, Aragón-Calvo MA, Forero-Romero JE, Gonzalez R, Gottlöber S, Hahn O, Hellwing WA, Hoffman Y, Jones BJT, Kitaura F, Knebe A, Manti S, Neyrinck M, Nuza SE, Padilla N, Platen E, Ramachandra N, Robotham A, Saar E, Shandarin S, Steinmetz M, Stoica RS, Sousbie T and Yepes G (2018), Jan. Tracing the cosmic web. *MNRAS* 473 (1): 1195–1217. doi:10.1093/mnras/stx1976. 1705.03021.

Linde AD (1983), Sep. Chaotic inflation. *Physics Letters B* 129 (3-4): 177–181. doi:10.1016/0370-2693(83)90837-7.

Lombriser L, Slosar A, Seljak U and Hu W (2012), Jun. Constraints on f(R) gravity from probing the large-scale structure. *Phys. Rev. D* 85 (12), 124038. doi:10.1103/PhysRevD.85.124038. 1003.3009.

Mao Q, Berlind AA, Scherrer RJ, Neyrinck MC, Scoccimarro R, Tinker JL, McBride CK, Schneider DP, Pan K, Bizyaev D, Malanushenko E and Malanushenko V (2017), Feb. A Cosmic Void Catalog of SDSS DR12 BOSS Galaxies. *ApJ* 835, 161. doi:10.3847/1538-4357/835/2/161. 1602.02771.

Massara E and Sheth RK (2018), Nov. Density and velocity profiles around cosmic voids. *arXiv e-prints* , arXiv:1811.03132doi:10.48550/arXiv.1811.03132. 1811.03132.

Massara E, Villaescusa-Navarro F, Viel M and Sutter PM (2015), Nov. Voids in massive neutrino cosmologies. *JCAP* 11, 018. doi:10.1088/1475-7516/2015/11/018. 1506.03088.

Mauland R, Elgarøy Ø, Mota DF and Winther HA (2023), Jun. The void-galaxy cross-correlation function with massive neutrinos and modified gravity. *A&A* 674, A185. doi:10.1051/0004-6361/202346287. 2303.05820.

Mazurenko S, Banik I and Kroupa P (2025), Feb. The redshift dependence of the inferred H_0 in a local void solution to the Hubble tension. *MNRAS* 536 (4): 3232–3241. doi:10.1093/mnras/stae2758. 2412.12245.

Melchior P, Sutter PM, Sheldon ES, Krause E and Wandelt BD (2014), Jun. First measurement of gravitational lensing by cosmic voids in SDSS. *MNRAS* 440: 2922–2927. doi:10.1093/mnras/stu456. 1309.2045.

Nadathur S (2016), Sep. Testing cosmology with a catalogue of voids in the BOSS galaxy surveys. *MNRAS* 461: 358–370. doi:10.1093/mnras/stw1340. 1602.04752.

Nadathur S and Crittenden R (2016), Oct. A Detection of the Integrated Sachs-Wolfe Imprint of Cosmic Superstructures Using a Matched-filter Approach. *ApJ* 830, L19. doi:10.3847/2041-8205/830/1/L19. 1608.08638.

Nadathur S and Percival WJ (2017), Dec. An accurate linear model for redshift space distortions in the void-galaxy correlation function. *ArXiv e-prints* 1712.07575.

Nadathur S, Hotchkiss S and Sarkar S (2012), Jun. The integrated Sachs-Wolfe imprint of cosmic superstructures: a problem for ΛCDM. *JCAP* 6, 042. doi:10.1088/1475-7516/2012/06/042. 1109.4126.

Nadathur S, Carter P and Percival WJ (2019a), Jan. A Zeldovich reconstruction method for measuring redshift space distortions using cosmic

voids. *MNRAS* 482 (2): 2459–2470. doi:10.1093/mnras/sty2799. 1805.09349.

Nadathur S, Carter PM, Percival WJ, Winther HA and Bautista JE (2019b), Jul. Beyond BAO: Improving cosmological constraints from BOSS data with measurement of the void-galaxy cross-correlation. *Phys. Rev. D* 100 (2), 023504. doi:10.1103/PhysRevD.100.023504. 1904.01030.

Nadathur S, Woodfinden A, Percival WJ, Aubert M, Bautista J, Dawson K, Escoffier S, Fromenteau S, Gil-Marín H, Rich J, Ross AJ, Rossi G, Magaña MV, Brownstein JR and Schneider DP (2020), Dec. The completed SDSS-IV extended baryon oscillation spectroscopic survey: geometry and growth from the anisotropic void-galaxy correlation function in the luminous red galaxy sample. *MNRAS* 499 (3): 4140–4157. doi:10.1093/mnras/staa3074. 2008.06060.

Neyrinck MC (2008), Jun. ZOBOV: a parameter-free void-finding algorithm. *MNRAS* 386: 2101–2109. doi:10.1111/j.1365-2966.2008.13180.x. 0712.3049.

Neyrinck MC and Yang LF (2013), Aug. Ringing the initial Universe: the response of overdensity and transformed-density power spectra to initial spikes. *MNRAS* 433 (2): 1628–1633. doi:10.1093/mnras/stt949. 1305.1629.

Neyrinck MC, Hidding J, Konstantatou M and van de Weygaert R (2018), Apr. The cosmic spiderweb: equivalence of cosmic, architectural and origami tessellations. *Royal Society Open Science* 5 (4), 171582. doi:10.1098/rsos.171582. 1710.04509.

Neyrinck M, Genel S and Stücker J (2022), Jun. Boundaries of chaos and determinism in the cosmos. *arXiv e-prints* , arXiv:2206.10666doi: 10.48550/arXiv.2206.10666. 2206.10666.

Padilla ND, Ceccarelli L and Lambas DG (2005), Nov. Spatial and dynamical properties of voids in a Λ cold dark matter universe. *MNRAS* 363: 977–990. doi:10.1111/j.1365-2966.2005.09500.x. astro-ph/0508297.

Paillas E, Cautun M, Li B, Cai YC, Padilla N, Armijo J and Bose S (2019), Mar. The Santiago-Harvard-Edinburgh-Durham void comparison II: unveiling the Vainshtein screening using weak lensing. *MNRAS* 484 (1): 1149–1165. doi:10.1093/mnras/stz022. 1810.02864.

Paillas E, Cai YC, Padilla N and Sánchez AG (2021), Aug. Redshift-space distortions with split densities. *MNRAS* 505 (4): 5731–5752. doi: 10.1093/mnras/stab1654. 2101.09854.

Pan DC, Vogeley MS, Hoyle F, Choi YY and Park C (2012), Apr. Cosmic voids in Sloan Digital Sky Survey Data Release 7. *MNRAS* 421: 926–934. doi:10.1111/j.1365-2966.2011.20197.x. 1103.4156.

Paz D, Lares M, Ceccarelli L, Padilla N and Lambas DG (2013), Dec. Clues on void evolution-II. Measuring density and velocity profiles on SDSS galaxy redshift space distortions. *MNRAS* 436 (4): 3480–3491. doi:10.1093/mnras/stt1836. 1306.5799.

Paz DJ, Correa CM, Gualpa SR, Ruiz AN, Bederián CS, Graña RD and Padilla ND (2023), Jun. Guess the cheese flavour by the size of its holes: a cosmological test using the abundance of popcorn voids. *MNRAS* 522 (2): 2553–2569. doi:10.1093/mnras/stad1146. 2212.06849.

Peebles PJE (1980). The large-scale structure of the universe.

Peebles PJE and Nusser A (2010), Jun. Nearby galaxies as pointers to a better theory of cosmic evolution. *Nature* 465 (7298): 565–569. doi:10.1038/nature09101. 1001.1484.

Pelliciari D, Contarini S, Marulli F, Moscardini L, Giocoli C, Lesci GF and Dolag K (2023), Jun. Exploring the cosmological synergy between galaxy cluster and cosmic void number counts. *MNRAS* 522 (1): 152–164. doi:10.1093/mnras/stad956. 2210.07248.

Perico ELD, Voivodic R, Lima M and Mota DF (2019), May. Cosmic voids in modified gravity scenarios. *arXiv e-prints* , arXiv:1905.12450doi: 10.48550/arXiv.1905.12450. 1905.12450.

Planck Collaboration, Ade PAR, Aghanim N, Armitage-Caplan C, Arnaud M, Ashdown M, Atrio-Barandela F, Aumont J, Baccigalupi C, Banday AJ, Barreiro RB, Bartlett JG, Basak S, Battaner E, Benabed K, Benoît A, Benoit-Lévy A, Bernard JP, Bersanelli M, Bielewicz P, Bobin J, Bock JJ, Bonaldi A, Bonavera L, Bond JR, Borrill J, Bouchet FR, Bridges M, Bucher M, Burigana C, Butler RC, Cardoso JF, Catalano A, Challinor A, Chamballu A, Chiang HC, Chiang LY, Christensen PR, Church S, Clements DL, Colombi S, Colombo LPL, Couchot F, Coulais A, Crill BP, Curto A, Cuttaia F, Danese L, Davies RD, Davis RJ, de Bernardis P, de Rosa A, de Zotti G, Déchelette T, Delabrouille J, Delouis JM, Désert FX, Dickinson C, Diego JM, Dole H, Donzelli S, Doré O, Douspis M, Dunkley J, Dupac X, Efstathiou G, Enßlin TA, Eriksen HK, Finelli F, Forni O, Frailis M, Franceschi E, Galeotta S, Ganga K, Giard M, Giardino G, Giraud-Héraud Y, González-Nuevo J, Górski KM, Gratton S, Gregorio A, Gruppuso A, Gudmundsson JE, Hansen FK, Hanson D, Harrison D, Henrot-Versillé S, Hernández-Monteagudo C, Herranz D, Hildebrandt SR, Hivon E, Ho S, Hobson M, Holmes WA, Hornstrup A, Hovest W, Huffenberger KM, Jaffe AH, Jaffe TR, Jones WC, Juvela M, Keihänen E, Keskitalo R, Kisner TS, Kneissl R, Knoche J, Knox L, Kunz M, Kurki-Suonio H, Lagache G, Lähteenmäki A, Lamarre JM, Lasenby A, Laureijs RJ, Lavabre A, Lawrence CR, Leahy JP, Leonardi R, León-Tavares J, Lesgourgues J, Lewis A, Liguori M, Lilje PB, Linden-Vørnle M, López-Caniego M, Lubin PM, Macías-Pérez JF, Maffei B, Maino D, Mandolesi N, Mangilli A, Maris M, Marshall DJ, Martin PG, Martínez-González E, Masi S, Massardi M, Matarrese S, Matthai F, Mazzotta P, Melchiorri A, Mendes L, Mennella A, Migliaccio M, Mitra S, Miville-Deschênes MA, Moneti A, Montier L, Morgante G, Mortlock D, Moss A, Munshi D, Murphy JA, Naselsky P, Nati F, Natoli P, Netterfield CB, Nørgaard-Nielsen HU, Noviello F, Novikov D, Novikov I, Osborne S, Oxborrow CA, Paci F, Pagano L, Pajot F, Paoletti D, Partridge B, Pasian F, Patanchon G, Perdereau O, Perotto L, Perrotta F, Piacentini F, Piat M, Pierpaoli E, Pietrobon D, Plaszczynski S, Pointecouteau E, Polenta G, Ponthieu N, Popa L, Poutanen T, Pratt GW, Prézeau G, Prunet S, Puget JL, Pullen AR, Rachen JP, Rebolo R, Reinecke M, Remazeilles M, Renault C, Ricciardi S, Riller T, Ristorcelli I, Rocha G, Rosset C, Roudier G, Rowan-Robinson M, Rubiño-Martín JA, Rusholme B, Sandri M, Santos D, Savini G, Scott D, Seiffert MD, Shellard EPS, Smith K, Spencer LD, Starck JL, Stolyarov V, Stompor R, Sudiwala R, Sunyaev R, Sureau F, Sutton D, Suur-Uski AS, Sygnet JF, Tauber JA, Tavagnacco D, Terenzi L, Toffolatti L, Tomasi M, Tristram M, Tucci M, Tuovinen J, Umana G, Valenziano L, Valiviita J, Van Tent B, Vielva P, Villa F, Vittorio N, Wade LA, Wandelt BD, White M, White SDM, Yvon D, Zacchei A and Zonca A (2014), Nov. Planck 2013 results. XVII. Gravitational lensing by large-scale structure. *A&A* 571, A17. doi:10.1051/0004-6361/201321543. 1303.5077.

Planck Collaboration, Ade PAR, Aghanim N, Arnaud M, Ashdown M, Aumont J, Baccigalupi C, Banday AJ, Barreiro RB, Bartolo N and et al. (2016), Sep. Planck 2015 results. XXI. The integrated Sachs-Wolfe effect. *A&A* 594, A21. doi:10.1051/0004-6361/201525831. 1502.01595.

Platen E, van de Weygaert R and Jones BJT (2007), Sep. A cosmic watershed: the WVF void detection technique. *MNRAS* 380: 551–570. doi:10.1111/j.1365-2966.2007.12125.x. 0706.2788.

Press WH and Schechter P (1974), Feb. Formation of Galaxies and Clusters of Galaxies by Self-Similar Gravitational Condensation. *ApJ* 187: 425–438. doi:10.1086/152650.

Rácz G, Dobos L, Beck R, Szapudi I and Csabai I (2017), Jul. Concordance cosmology without dark energy. *MNRAS* 469 (1): L1–L5. doi: 10.1093/mnrasl/slx026. 1607.08797.

Radinović S, Nadathur S, Winther HA, Percival WJ, Woodfinden A, Massara E, Paillas E, Contarini S, Hamaus N, Kovacs A, Pisani A, Verza G, Aubert M, Amara A, Auricchio N, Baldi M, Bonino D, Branchini E, Brescia M, Camera S, Capobianco V, Carbone C, Cardone VF, Carretero J, Castellano M, Cavuoti S, Cimatti A, Cledassou R, Congedo G, Conversi L, Copin Y, Corcione L, Courbin F, Da Silva A, Douspis M, Dubath F, Dupac X, Farrens S, Ferriol S, Fosalba P, Frailis M, Franceschi E, Fumana M, Galeotta S, Garilli B, Gillard W, Gillis B, Giocoli C, Grazian A, Grupp F, Haugan SVH, Holmes W, Hornstrup A, Jahnke K, Kümmel M, Kiessling A, Kilbinger M, Kitching T, Kurki-Suonio H, Ligori S, Lilje PB, Lloro I, Maiorano E, Mansutti O, Marggraf O, Markovic K, Marulli F, Massey R, Mei S, Melchior M, Mellier Y, Meneghetti M, Merlin E, Meylan G, Moresco M, Moscardini L, Niemi SM, Nightingale JW, Nutma T, Padilla C, Paltani S, Pasian F, Pedersen K, Pettorino V, Pires S, Polenta G, Poncet M, Popa LA, Pozzetti L, Raison F, Renzi A, Rhodes J, Riccio G, Romelli E, Roncarelli M, Rosset C, Saglia R, Sapone D, Sartoris B,

Schneider P, Secroun A, Seidel G, Serrano S, Sirignano C, Sirri G, Stanco L, Starck JL, Surace C, Tallada-Crespí P, Tereno I, Toledo-Moreo R, Torradeflot F, Tutusaus I, Valentijn EA, Valenziano L, Vassallo T, Wang Y, Weller J, Zamorani G, Zoubian J and Scottez V (2023), Sep. Euclid: Cosmology forecasts from the void-galaxy cross-correlation function with reconstruction. *A&A* 677, A78. doi:10.1051/0004-6361/202346121. 2302.05302.

Raghunathan S, Nadathur S, Sherwin BD and Whitehorn N (2020), Feb. The Gravitational Lensing Signatures of BOSS Voids in the Cosmic Microwave Background. *ApJ* 890 (2), 168. doi:10.3847/1538-4357/ab6f05. 1911.08475.

Renk J, Zumalacárregui M, Montanari F and Barreira A (2017), Oct. Galileon gravity in light of ISW, CMB, BAO and H_0 data. *JCAP* 2017 (10), 020. doi:10.1088/1475-7516/2017/10/020. 1707.02263.

Reyes R, Mandelbaum R, Seljak U, Baldauf T, Gunn JE, Lombriser L and Smith RE (2010), Mar. Confirmation of general relativity on large scales from weak lensing and galaxy velocities. *Nature* 464: 256–258. doi:10.1038/nature08857. 1003.2185.

Ronconi T and Marulli F (2017), Oct. Cosmological exploitation of cosmic void statistics. New numerical tools in the CosmoBolognaLib to extract cosmological constraints from the void size function. *A&A* 607, A24. doi:10.1051/0004-6361/201730852. 1703.07848.

Ronconi T, Contarini S, Marulli F, Baldi M and Moscardini L (2019), Oct. Cosmic voids uncovered - first-order statistics of depressions in the biased density field. *MNRAS* 488 (4): 5075–5084. doi:10.1093/mnras/stz2115. 1902.04585.

Sachs RK and Wolfe AM (1967), Jan. Perturbations of a Cosmological Model and Angular Variations of the Microwave Background. *ApJ* 147: 73. doi:10.1086/148982.

Sahlén M (2019), Mar. Cluster-void degeneracy breaking: Neutrino properties and dark energy. *Phys. Rev. D* 99 (6), 063525. doi:10.1103/PhysRevD.99.063525. 1807.02470.

Sahlén M and Silk J (2016), Dec. Cluster-Void Degeneracy Breaking: Modified Gravity in the Balance. *ArXiv e-prints* 1612.06595.

Sahlén M, Zubeldía Í and Silk J (2016), Mar. Cluster-Void Degeneracy Breaking: Dark Energy, Planck, and the Largest Cluster and Void. *ApJ* 820, L7. doi:10.3847/2041-8205/820/1/L7. 1511.04075.

Sánchez C, Clampitt J, Kovacs A, Jain B, García-Bellido J, Nadathur S, Gruen D, Hamaus N, Huterer D, Vielzeuf P, Amara A, Bonnett C, DeRose J, Hartley WG, Jarvis M, Lahav O, Miquel R, Rozo E, Rykoff ES, Sheldon E, Wechsler RH, Zuntz J, Abbott TMC, Abdalla FB, Annis J, Benoit-Lévy A, Bernstein GM, Bernstein RA, Bertin E, Brooks D, Buckley-Geer E, Carnero Rosell A, Carrasco Kind M, Carretero J, Crocce M, Cunha CE, D'Andrea CB, da Costa LN, Desai S, Diehl HT, Dietrich JP, Doel P, Evrard AE, Fausti Neto A, Flaugher B, Fosalba P, Frieman J, Gaztanaga E, Gruendl RA, Gutierrez G, Honscheid K, James DJ, Krause E, Kuehn K, Lima M, Maia MAG, Marshall JL, Melchior P, Plazas AA, Reil K, Romer AK, Sanchez E, Schubnell M, Sevilla-Noarbe I, Smith RC, Soares-Santos M, Sobreira F, Suchyta E, Tarle G, Thomas D, Walker AR, Weller J and DES Collaboration (2017), Feb. Cosmic voids and void lensing in the Dark Energy Survey Science Verification data. *MNRAS* 465: 746–759. doi:10.1093/mnras/stw2745. 1605.03982.

Shandarin S, Habib S and Heitmann K (2012), Apr. Cosmic web, multistream flows, and tessellations. *Phys. Rev. D* 85 (8), 083005. doi:10.1103/PhysRevD.85.083005. 1111.2366.

Shanks T, Hogarth LM and Metcalfe N (2019), Mar. Gaia Cepheid parallaxes and 'Local Hole' relieve H_0 tension. *MNRAS* 484 (1): L64–L68. doi:10.1093/mnrasl/sly239. 1810.02595.

Sheth RK and van de Weygaert R (2004), May. A hierarchy of voids: much ado about nothing. *MNRAS* 350: 517–538. doi:10.1111/j.1365-2966.2004.07661.x. astro-ph/0311260.

Singh S, Alam S, Mandelbaum R, Seljak U, Rodriguez-Torres S and Ho S (2018), Mar. Probing gravity with a joint analysis of galaxy and CMB lensing and SDSS spectroscopy. *ArXiv e-prints* 1803.08915.

Skara F and Perivolaropoulos L (2020), Mar. Tension of the E_G statistic and redshift space distortion data with the Planck-Λ CDM model and implications for weakening gravity. *Phys. Rev. D* 101 (6), 063521. doi:10.1103/PhysRevD.101.063521. 1911.10609.

Song YS, Peiris H and Hu W (2007), Sep. Cosmological constraints on f(R) acceleration models. *Phys. Rev. D* 76 (6), 063517. doi:10.1103/PhysRevD.76.063517. 0706.2399.

Song Y, Xiong Q, Gong Y, Deng F, Chan KC, Chen X, Guo Q, Han J, Li G, Li M, Liu Y, Luo Y, Pei W and Wei C (2024), Jul. Cosmological forecast of the void size function measurement from the CSST spectroscopic survey. *MNRAS* 532 (1): 1049–1058. doi:10.1093/mnras/stae1575. 2402.05492.

Spolyar D, Sahlén M and Silk J (2013), Dec. Topology and Dark Energy: Testing Gravity in Voids. *Physical Review Letters* 111 (24), 241103. doi:10.1103/PhysRevLett.111.241103. 1304.5239.

Springel V, White SDM, Jenkins A, Frenk CS, Yoshida N, Gao L, Navarro J, Thacker R, Croton D, Helly J, Peacock JA, Cole S, Thomas P, Couchman H, Evrard A, Colberg J and Pearce F (2005), Jun. Simulations of the formation, evolution and clustering of galaxies and quasars. *Nature* 435 (7042): 629–636. doi:10.1038/nature03597. astro-ph/0504097.

Stücker J, Busch P and White SDM (2018), Jul. The median density of the Universe. *MNRAS* 477 (3): 3230–3246. doi:10.1093/mnras/sty815. 1710.09881.

Su C, Shan H, Zhang J, Zhao C, Yu J, Wang Q, Xiao L, Liu X and Zhao A (2023), Jul. Void Lensing in Cubic Galileon Gravity. *ApJ* 951 (1), 64. doi:10.3847/1538-4357/acd63d. 2211.10187.

Sunyaev RA and Zeldovich YB (1970), Apr. Small-Scale Fluctuations of Relic Radiation. *Ap&SS* 7 (1): 3–19. doi:10.1007/BF00653471.

Sunyaev RA and Zeldovich IB (1980a), Jan. Microwave background radiation as a probe of the contemporary structure and history of the universe. *ARA&A* 18: 537–560. doi:10.1146/annurev.aa.18.090180.002541.

Sunyaev RA and Zeldovich YB (1980b), Feb. The velocity of clusters of galaxies relative to the microwave background - The possibility of its measurement. *MNRAS* 190: 413–420. doi:10.1093/mnras/190.3.413.

Sutter PM, Lavaux G, Wandelt BD and Weinberg DH (2012), Dec. A Public Void Catalog from the SDSS DR7 Galaxy Redshift Surveys Based on the Watershed Transform. *ApJ* 761, 44. doi:10.1088/0004-637X/761/1/44. 1207.2524.

Sutter PM, Carlesi E, Wandelt BD and Knebe A (2015), Jan. On the observability of coupled dark energy with cosmic voids. *MNRAS* 446: L1–L5. doi:10.1093/mnrasl/slu155. 1406.0511.

Szalay A and Marx G (1976). Neutrino rest mass from cosmology. *Astronomy and Astrophysics, vol. 49, no. 3, June 1976, p. 437-441.* 49: 437–441.

Szapudi I, Kovács A, Granett BR, Frei Z, Silk J, Burgett W, Cole S, Draper PW, Farrow DJ, Kaiser N, Magnier EA, Metcalfe N, Morgan JS, Price P, Tonry J and Wainscoat R (2015), Jun. Detection of a supervoid aligned with the cold spot of the cosmic microwave background. *MNRAS* 450 (1): 288–294. doi:10.1093/mnras/stv488. 1405.1566.

Tamone A, Zhao C, Forero-Sánchez D, Variu A, Chuang CH, Kitaura FS, Kneib JP and Tao C (2023), Dec. Void BAO measurements on quasars from eBOSS. *MNRAS* 526 (2): 2889–2902. doi:10.1093/mnras/stad2898. 2208.06238.

Thiele L, Massara E, Pisani A, Hahn C, Spergel DN, Ho S and Wandelt B (2024), Jul. Neutrino Mass Constraint from an Implicit Likelihood Analysis of BOSS Voids. *ApJ* 969 (2), 89. doi:10.3847/1538-4357/ad434e. 2307.07555.

Tully RB and Fisher JR (1987). Nearby Galaxies Atlas, Cambridge University Press, Cambridge, UK.

Tully RB, Pomarède D, Graziani R, Courtois HM, Hoffman Y and Shaya EJ (2019), Jul. Cosmicflows-3: Cosmography of the Local Void. *ApJ* 880

(1), 24. doi:10.3847/1538-4357/ab2597. 1905.08329.

van de Weygaert R (2016), Oct., Voids and the Cosmic Web: cosmic depression & spatial complexity, van de Weygaert R, Shandarin S, Saar E and Einasto J, (Eds.), The Zeldovich Universe: Genesis and Growth of the Cosmic Web, IAU Symposium, 308, 493–523, 1611.01222.

Verza G, Carbone C, Pisani A, Porciani C and Matarrese S (2024), Oct. The universal multiplicity function: counting haloes and voids. *JCAP* 2024 (10), 079. doi:10.1088/1475-7516/2024/10/079. 2401.14451.

Vielzeuf P, Kovács A, Demirbozan U, Fosalba P, Baxter E, Hamaus N, Huterer D, Miquel R, Nadathur S, Pollina G, Sánchez C, Whiteway L, Abbott TMC, Allam S, Annis J, Avila S, Brooks D, Burke DL, Carnero Rosell A, Carrasco Kind M, Carretero J, Cawthon R, Costanzi M, da Costa LN, De Vicente J, Desai S, Diehl HT, Doel P, Eifler TF, Everett S, Flaugher B, Frieman J, García-Bellido J, Gaztanaga E, Gerdes DW, Gruen D, Gruendl RA, Gschwend J, Gutierrez G, Hartley WG, Hollowood DL, Honscheid K, James DJ, Kuehn K, Kuropatkin N, Lahav O, Lima M, Maia MAG, March M, Marshall JL, Melchior P, Menanteau F, Palmese A, Paz-Chinchón F, Plazas AA, Sanchez E, Scarpine V, Serrano S, Sevilla-Noarbe I, Smith M, Suchyta E, Tarle G, Thomas D, Weller J, Zuntz J, Zuntz J and DES Collaboration (2021), Jan. Dark Energy Survey Year 1 results: the lensing imprint of cosmic voids on the cosmic microwave background. *MNRAS* 500 (1): 464–480. doi:10.1093/mnras/staa3231. 1911.02951.

Vielzeuf P, Calabrese M, Carbone C, Fabbian G and Baccigalupi C (2023), Aug. DEMNUni: the imprint of massive neutrinos on the cross-correlation between cosmic voids and CMB lensing. *JCAP* 2023 (8), 010. doi:10.1088/1475-7516/2023/08/010. 2303.10048.

Vogeley MS, Geller MJ and Huchra JP (1991), Nov. Void Statistics of the CfA Redshift Survey. *ApJ* 382: 44. doi:10.1086/170691.

Voivodic R, Lima M, Llinares C and Mota DF (2017), Jan. Modeling void abundance in modified gravity. *Phys. Rev. D* 95 (2), 024018. doi:10.1103/PhysRevD.95.024018. 1609.02544.

Wenzl L, Bean R, Chen SF, Farren GS, Madhavacheril MS, Marques GA, Qu FJ, Sehgal N, Sherwin BD and van Engelen A (2024), Apr. Constraining gravity with a new precision E_G estimator using Planck + SDSS BOSS data. *Phys. Rev. D* 109 (8), 083540. doi:10.1103/PhysRevD.109.083540. 2401.12971.

Whitbourn JR and Shanks T (2014), Jan. The local hole revealed by galaxy counts and redshifts. *MNRAS* 437 (3): 2146–2162. doi:10.1093/mnras/stt2024. 1307.4405.

White SDM (1979), Jan. The hierarchy of correlation functions and its relation to other measures of galaxy clustering. *MNRAS* 186: 145–154. doi:10.1093/mnras/186.2.145.

Wilson C and Bean R (2023), Jun. Challenges in constraining gravity with cosmic voids. *Phys. Rev. D* 107 (12), 124008. doi:10.1103/PhysRevD.107.124008. 2212.02569.

Wiltshire DL (2009), Dec. Average observational quantities in the timescape cosmology. *Phys. Rev. D* 80 (12), 123512. doi:10.1103/PhysRevD.80.123512. 0909.0749.

Woodfinden A, Nadathur S, Percival WJ, Radinovic S, Massara E and Winther HA (2022), Nov. Measurements of cosmic expansion and growth rate of structure from voids in the Sloan Digital Sky Survey between redshift 0.07 and 1.0. *MNRAS* 516 (3): 4307–4323. doi:10.1093/mnras/stac2475. 2205.06258.

Woodfinden A, Percival WJ, Nadathur S, Winther HA, Fraser TS, Massara E, Paillas E and Radinović S (2023), Aug. Cosmological measurements from void-galaxy and galaxy-galaxy clustering in the Sloan Digital Sky Survey. *MNRAS* 523 (4): 6360–6370. doi:10.1093/mnras/stad1725. 2303.06143.

Yang LF, Neyrinck MC, Aragón-Calvo MA, Falck B and Silk J (2015), Aug. Warmth elevating the depths: shallower voids with warm dark matter. *mnras* 451: 3606–3614. doi:10.1093/mnras/stv1087. 1411.5029.

Zentner AR (2007). The Excursion Set Theory of Halo Mass Functions, Halo Clustering, and Halo Growth. *International Journal of Modern Physics D* 16: 763–815. doi:10.1142/S0218271807010511. astro-ph/0611454.

Zhang P and Stebbins A (2011), Jul. Confirmation of the Copernican Principle at Gpc Radial Scale and above from the Kinetic Sunyaev-Zel'dovich Effect Power Spectrum. *Phys. Rev. Lett.* 107 (4), 041301. doi:10.1103/PhysRevLett.107.041301. 1009.3967.

Zhang P, Liguori M, Bean R and Dodelson S (2007), Oct. Probing Gravity at Cosmological Scales by Measurements which Test the Relationship between Gravitational Lensing and Matter Overdensity. *Physical Review Letters* 99 (14), 141302. doi:10.1103/PhysRevLett.99.141302. 0704.1932.

Zhang G, Li Z, Liu J, Spergel DN, Kreisch CD, Pisani A and Wandelt BD (2020), Oct. Void halo mass function: A promising probe of neutrino mass. *Phys. Rev. D* 102 (8), 083537. doi:10.1103/PhysRevD.102.083537. 1910.07553.

Zhao C, Chuang CH, Kitaura FS, Liang Y, Pellejero-Ibanez M, Tao C, Vargas-Magaña M, Variu A and Yepes G (2020), Jan. Improving baryon acoustic oscillation measurement with the combination of cosmic voids and galaxies. *MNRAS* 491 (3): 4554–4572. doi:10.1093/mnras/stz3339. 1802.03990.

Zhao C, Variu A, He M, Forero-Sánchez D, Tamone A, Chuang CH, Kitaura FS, Tao C, Yu J, Kneib JP, Percival WJ, Shan H, Zhao GB, Burtin E, Dawson KS, Rossi G, Schneider DP and de la Macorra A (2022), Apr. The completed SDSS-IV extended Baryon Oscillation Spectroscopic Survey: cosmological implications from multitracer BAO analysis with galaxies and voids. *MNRAS* 511 (4): 5492–5524. doi:10.1093/mnras/stac390. 2110.03824.